Received: 31 October 2022 | Revised: 27 December 2022 | Accepted: 17 January 2023

IET Generation, Transmission & Distribution

DOI: 10.1049/gtd2.12778

The Institution of Engineering and Technology WILEY

REVIEW

A survey of sag monitoring methods for power grid transmission lines

Yunfei Chen[1] | Xiaolin Ding[2]

[1]The Department of Engineering, University of Durham, Durham, UK

[2]National Grid Electricity Transmission, Warwick, UK

Correspondence
Yunfei Chen, The Department of Engineering, University of Durham, Durham, DH1 3LE, UK.
Email: Yunfei.Chen@durham.ac.uk

Funding information
National Grid, Grant/Award Number: NIA2_NGET0013

Abstract

The transmission line is a fundamental asset in the power grid. The sag condition of the transmission line between two support towers requires accurate real-time monitoring in order to avoid any health and safety hazards or power failure. In this paper, state-of-the-art methods on transmission line sag monitoring are thoroughly reviewed and compared. Both the direct methods that use the direct video or image of the transmission line and the indirect methods that use the relationships between sag and line parameters are investigated. Sag prediction methods and relevant industry standards are also examined. Based on these investigation and examination, future research challenges are outlined and useful recommendations on the choices of sag monitoring methods in different applications are made.

1 | INTRODUCTION

Transmission line is an integral and important part of the power grid that connects the power plants at the generation end to the consumers at the distribution end. Its reliability is of utmost importance, as any disturbance or failure in the transmission line could lead to significant and large-scale disruption of the power supply. On the other hand, due to the fast pace and growing pressure of the transition to low carbon economy from governments around the world, the electricity network has to integrate bulk renewable connections to meet future energy needs. This necessitates a significant increase in power transfer capability in the transmission network. Considering the cost, long lead time and challenges in planning and consents for building new transmission lines, it is more economical to maximise the power transfer capability of the existing circuits. Therefore, many transmission owners have explored ways to unlock/increase the transfer capacity of existing transmission lines, in addition to building new lines [1].

An increased power transfer capability closely correlates with an increased current in the transmission lines. However, an increase in current could lead to an increase in temperature, which could consequently expand or distort the transmission lines from their designed limits and cause potential risks to the network as well as properties and humans near the network. For example, in 2003, a large blackout happened in the US and part of Canada affecting more than 50 million people, which was believed to be caused by overloaded transmission lines that drooped into foliage [2]. In addition to this, snow, icing, wind and other factors could all lead to unexpected events in the transmission lines and the power network as a whole by changing the sagging conditions of the lines [3].

In the UK, the transmission lines mainly operate at 400 kV and 275 kV, while the distribution lines operate at 132 kV, 33 kV, 11 kV and 230 V, for transfer efficiency. To protect the safety of the general public and ground properties, the transmission lines need to be at least 5.2 m above the ground according to the UK Electricity Safety, Quality and Continuity Regulations 2002 17(2) Schedule 2. Consequently, most transmission towers in the UK have a height between 15 and 55 m and most of them are located in remote areas. The high voltage and remote location of the transmission lines make it difficult to monitor their status in real-time.

Different types of conductors are used as transmission lines to transfer electricity. Their selection depends on their sizes, electrical and mechanical properties. In general, they can be classified as homogeneous conductors that use the same strand material and composite conductors that mix strands of wires with different materials for better electrical and mechanical properties. A good conductor can not

only increase the power transfer capacity but also operate at a higher temperature with lower sag by using new materials [4]. The conventional composite conductors include all aluminium conductor (AAC), all aluminium alloy conductor (AAAC), aluminium-conductor alloy-reinforced (ACAR), aluminium conductor-steel reinforced (ACSR) and aluminium alloy conductor steel-reinforced (AACSR). They contain all-aluminium alloy strands, while the aluminium core of the strands is replaced by other core materials, such as steel or alloy, to improve the electrical and mechanical properties. For example, aluminium wire has a high thermal expansion coefficient, giving faster expansion of the core strand when it is exposed to a high temperature. Among them, ACSR has several advantages and is widely used.

Recently, conventional composite conductors have been modified to improve their power transfer performance by using different types of coating for corrosion resistance, deformation of strand shape, and changing the geometric configuration of the conductor. These modifications aim to improve their electrical and mechanical properties to strengthen their ability to resist strong wind (galloping), low wind speed (Aeolian vibration), ice loading, and high temperatures. The high-temperature low sag (HTLS) conductors thus became a good choice in recent years. It operates at a temperature of between 150° to 250°, much higher than conventional conductors. Also, it is able to address the vibration and galloping issues and increase the power capacity of transmission lines to meet the increasing electricity demand. It also has less weight, less sag and more strength compared with ACSR.

In general, overhead line sag is defined as the distance from the straight line connecting two support towers to the lowest point of the transmission line. It is an important state parameter of the transmission line and is directly related to the ground clearance (which is the difference between the height of support towers and the sag of the line). Sag is deliberately introduced into the transmission line for safety reasons.

- Tension: When a transmission line is held by two towers, tension will be generated and if the tension is above a certain limit, either the transmission line could be broken or the transmission towers could be tilted. Hence, sag is closely related to tension, and the larger the sag is, the smaller the tension will be.
- Current: Sag depends on the current flowing through the transmission line. When the current in the line increases, the transmission line will be heated to expand its length. Consequently, this increases the sag.
- Length: When the length increases, the power transfer loss increases due to the increased reactance of the transmission line. This reduces the power transfer efficiency. Meanwhile, for the same span length, the sag also increases with the increase in length. Hence, the line length affects both the sag and the power transfer efficiency.
- Weather: Sag relies on weather conditions too. For example, ice will add weight to the transmission line to increase the sag. Wind could cause swings in the transmission lines that change the sag, while hot or cold weather affects the ambient temperature of the transmission line thus also affects sag directly.
- Clearance: To protect ground facilities and assets and also to prevent short-circuit caused by vegetation, and so on sag must be below a limit to maintain a reasonable clearance to the ground. Thus, the power line corridor clearance is vital.

In summary, the amount of sag in the overhead line has a huge impact on the allowable thermal capability of the line as well as the safety of the power network. The line sag must be maintained at clearance limits required by the regulators in all conditions. If one span of the line has a very small safety clearance margin to the ground, the current this span can carry will be restricted to prevent breaching the required clearance limits. Then this span will become a bottleneck in the network. It is therefore very important to monitor and measure the sag, preferably in real-time, for the best operation of power networks. If the sag of a line can be monitored in real-time, the remaining safety clearance margin can be understood and monitored frequently to fully explore the potential to operate the line with a higher power. Moreover, although the issue of sagging could be alleviated by using modified composite conductors or new materials, it is costly to replace all conductors in the existing network and the outage access required is challenging to obtain. Since sagging is also dynamic and dependent on the environment, one still needs to develop monitoring methods to measure them for safety.

A related topic to sag monitoring is dynamic thermal line rating [5]. The maximum power transfer capacity of the transmission line is usually limited by the heating consideration to keep them safe. Traditional networks often use static line rating, which is usually calculated using very conservative assumptions about the operating environment. This has greatly restricted the exploration of the full potential of transmission lines. The core of dynamic thermal line rating is to monitor the temperature of the transmission line in real-time instead of using conservative assumptions and then deliver the power based on the practical operating environment [6–8].

In this paper, the state-of-the-art methods for overhead transmission line sag monitoring will be surveyed. These methods either measure the line sagging directly using specialist equipment carried by different platforms, or take advantage of the relationships between sag and the electromagnetic/mechanical properties of the transmission lines to measure the line sagging indirectly using sophisticated signal processing software. These methods are compared in terms of their accuracy and their cost. Then, future research challenges on overhead line sag monitoring are outlined. To the best of the authors' knowledge, this is the most comprehensive survey on line sag monitoring to provide useful guidance and insights on how to select different methods for different requirements.

The rest of the paper is organised as follows: In Section 2, the direct methods for line sagging monitoring will be discussed. In Section 3, the indirect methods for line sagging monitoring will be reviewed. Section 4 will present the sag prediction methods, while Section 5 will present some commonly used sagging monitoring devices and relevant industrial standards. In

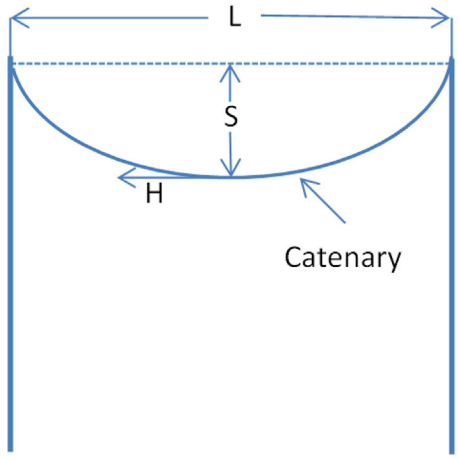

FIGURE 1 Sag for a levelled span.

Section 6, future research challenges on line sag monitoring will be examined and finally, Section 7 will conclude the paper.

2 | DIRECT METHODS

Due to its importance, sag monitoring has been well-studied since the power network was built more than a century ago. Figure 1 illustrates the sag for a levelled span, where S indicates the sag. Many monitoring methods have been developed in the past few decades to tackle this problem. These methods can be mainly categorized as direct methods and indirect methods. The direct methods often capture an image of the overhead line, either as a video sequence, 3D point cloud or a static picture, based on which the sag can be extracted through image processing or manual inspection by engineers. The indirect methods often measure some geometrical, electrical, magnetic or mechanical parameters of the overhead line, such as tension, temperature, space potential and magnetic flux density, and then use the theoretical or heuristic relationships between these parameters and the line sag to calculate the sag. In this section, the focus will be on the direct methods and in the next section, the indirect methods will be discussed.

As mentioned before, the direct methods capture an image of the overhead line to calculate the sag directly. Based on the platforms or sensors they use to capture the image, these can be aerial, terrestrial, line robots, cameras, GPS or other specially designed sensors. Aerial, terrestrial or line robots refer to the different platforms used to carry the sensors, while cameras or GPS refer to different sensors.

2.1 | Aerial

The aerial methods use either manned helicopters or unmanned aerial vehicles (UAVs) to take videos, laser scans or pictures of the overhead line, and then analyse images in these data for sag calculation via either manual inspection by humans or image processing by software. In some special applications, satellite imaging may also be used but in general, this method does not give good accuracy unless they use very expensive equipment or complicated image processing software. Hence, satellite imaging is not discussed here.

In [9], a camera was carried by a UAV to acquire images of the power line corridor for clearance detection. Using a series of images taken at slightly different times for the same power lines, decorrelation stretch was used for initial image processing, a modified Prewitt filter was used for edge enhancement, random sample consensus was used to line fitting, and epipolar geometry was used for 3D reconstruction. Digital surface model points intruding into the corridor were then detected by calculating the spatial distance between the reconstructed 3D power line and the point cloud representation of the corridor. Dangerous objects in the corridor were localised by segmenting points into voxels and subsequent clusterisation. This method was compared with terrestrial laser scanning and a total station survey. The accuracy of the 3D reconstruction for medium-power overhead lines was 15 cm and less than 30 cm for high-voltage lines.

In [10], a LIDAR was carried by helicopter to measure the distance between the overhead lines and nearby trees for a safety inspection. The LIDAR operated at a wavelength of 1.572 μm. An accuracy of 93 cm for the distance was obtained in their experiments for transmission lines of all voltages from 66 to 500 kV. This distance can be used to calculate the sag based on the position of the helicopter and the transmission lines.

In [11], another LIDAR was carried by a helicopter to extract the transmission line span from images created by laser return signals. A two-stage method was used, where the LIDAR data were first classified as transmission line, vegetation or surface, as they were the main objects that reflect the laser signals, and then the classified and extracted transmission line data were segmented into individual spans using local affine models to identify data points on the lines. It reported an accuracy of 86.9% for identifying data points on the transmission line and 72.1% for extracting the individual spans from the identified transmission lines.

Aerial LIDAR systems are useful to monitor the power line sagging but this method only captures the sagging of the transmission lines when and where the images were taken, while in practice the sagging could change dynamically with temperature and wind-induced swing so that lines at different locations in different times could have different sagging. This requires longer flights, which would increase the cost of the aerial methods. In [12], the authors simulated the dynamic positions of power lines under different weather conditions using point clouds based on mechanical computation. They considered the tension variation of lines due to weather conditions, such as temperature, wind, ice, and then simulated the line sag curve using the parabolic equation from tension. This method can model the dynamic position of the line with an error of less than 0.65 m.

In [13], a rod was placed on the transmission line as a target and then a UAV was used to take in-flight videos of the rod using a digital camera. From these videos, the 3D coordinates of the rod were measured using active vision technology. The error

between the actual coordinates of the rod and the calculated coordinates of the rod varies from 1.269% to 4.423% in different conditions. The sag was then calculated using non-linear least squares regression from the calculated 3D coordinates in the image. The error is small, but this method requires the installation of a rod on the transmission line and then a UAV flight to take images of the rod. This incurs a high cost for both equipment and outage access.

In [14], a 3D LIDAR was carried by a UAV to estimate the sag by combining the measured point cloud data from laser scanning with the flight information of the UAV. Again, a random sample consensus was used to extract point cloud data from the overhead line. The difference between the proposed method and manual inspection using 1D long-range LIDAR was between 3% and 5% for sag estimation. Similar work has been done in [15] using a 3D LIDAR carried by a UAV. With some additional image processing steps, the difference became 1.33% between the proposed method and the traditional total station method using a long-range 1D LIDAR. The inspection time has also been greatly reduced by using UAVs.

In [16], a camera carried by a UAV was used to take a single image of the transmission line based on which sag was calculated. First, contrast enhancement and threshold segmentation were used to obtain a binary image with a clear contour. Then, the connection points between the line and tower were selected as the interested points and an improved Harris detection algorithm was used to extract corner points and pixel coordinates. Then contour fitting of the transmission line was applied by using random circle, hyperbola and parabola fitting functions, and the best was chosen based on their root mean squared error. Finally, GPS and laser ranging were used to determine spatial distances between UAV and the transmission line, based on which sag was calculated. They reported an error as low as 0.38% for the sag calculation. This method combines almost all equipment required in the direct method, including UAV, GPS and LiDAR, and is the most expensive method in the literature, albeit its high accuracy. Hence, it is not suitable for large-scale deployment.

Remarks. One sees from the above that the aerial methods use either UAVs or helicopters to image the transmission lines as video, point cloud data or pictures and then calculate sag using image processing algorithms. Their performance largely relies on the efficiency of image processing algorithms applied, as well as the equipment used. From [14] and [15], the accuracy can be improved by using more image processing steps, while from [16], combining all equipment does give high accuracy.

2.2 | Terrestrial

The terrestrial methods are similar to the aerial methods, except that they perform sag monitoring on the ground rather than in the air. This certainly places some limitations on such methods. For example, some line spans may not be accessible from the ground due to vegetation or buildings, while other line spans in remote areas may be too far away to monitor from the ground. Nevertheless, terrestrial methods may be less expensive than aerial methods if labour cost is low.

In [17]–[23], infrared laser systems were used on the ground to measure the clearance and sag of overhead lines. The principle was to send an eye-safe infrared laser beam from a location near the line to the region where the lines were, and then scan it angularly on a plane perpendicular to the line to measure the elevation angle at which the laser signal was reflected from the conductor. Finally, using this angle and the distance from the monitor to the line, one can calculate the sag. In [17]–[19], the laser sag meter using an infrared source at 1550 nm was applied to calculate the sag and the clearance. Similar systems have been developed by the same authors for conductive defects [20], ice accumulation [21], winter icing and summer overheating [22, 23]. The accuracy is about 5 cm in most cases.

In [24], a terrestrial laser scanner Leica Scan Station P30 was used to extract the geometry of an overhead line for a span of 220 kV power line with a range of 300 m from the scanner. Point cloud data were obtained via scanning and then processed to extract the geometry, including the sag. The extracted geometry was compared with the theoretical models using the catenary and parabola equations. Their difference was less than 0.002 m in their settings. In [25], two optical sensors were used to measure the sag, where one sensor was mounted on the line and the other sensor was mounted on the tower. The distance between the two sensors and the angle to the horizontal line were calculated and using these two measurements and other known distances in the span, the sag of the overhead line were obtained.

In [26], a device called Nova OHLM system was developed to measure different parameters of the overhead line. It has several components, including a module installed on the overhead line for measuring current, temperature, inclination angle and so on, a digital camera and infrared illuminator installed on the tower for imaging and viewing of the overhead line, a module to measure the environment such as weather, solar radiation and ice, and a module providing the independent photovoltaic power supply. Sag was directly calculated using images from the digital camera. No accuracy was provided.

In [27], a camera was placed in front of the overhead line, not on the tower, to monitor icing and calculate sag. The camera took a picture of the transmission line. After background removal and contour detection, the smallest and largest x- and y-coordinates were calculated. The lowest point was then used to calculate the sag. No accuracy was provided. Similarly, in [28], a camera was placed close to the transmission line in a laboratory setting and the picture was converted to a binary image from which the shape of the line was extracted and sag can be calculated. The error was between +3% and -5%.

In [29], a digital camera was used to measure the static characteristics of the overhead line by computing the displacement of the line with respect to a known baseline position. Two high-speed digital cameras and a few markers mounted on the line were also used to calculate the dynamic characteristics by capturing two video sequences and then computing the 3D positions of a reference frame and displacements. Sags for different loading conditions were calculated. The error was about 0.03 mm.

In [30], a camera was installed on the tower to take pictures of the transmission lines for sag monitoring. It used the

hyperbolic cosine function to generate different templates tagged with different sagging values. Then, the test image was matched with different templates to measure the sag. The error can be as low as 0.13 cm using this method. In [31], a marker was placed on the overhead line, whose coordinates were captured by a camera and calculated using the direct linear transformation method. Similarly, reference [32] also used a camera to image the overhead line for sag calculation, except that the images were transmitted from the sensor to the ground via LoRa communications signals. A detailed review of computer vision or image processing techniques for sag monitoring using non-contact cameras can be found in [33]. In [34], a method similar to crowd sensing was used, where mobile phones from the general public were used to capture videos of overhead lines and shared with the system operators who then sampled images from these videos and converted them into augmented reality. No performance data was provided.

Remarks: The terrestrial method is one of the earliest and traditional methods developed. It relies on ground equipment and therefore is labour-intensive and suffers from many limitations, such as access, reliability and so on. Nevertheless, it is easy and simple to use. Image processing or human inspection are still required once the images are captured on the ground. Within the terrestrial methods, cameras are commonly available and a very useful sensor for sag monitoring, combined with computer vision or image processing algorithms. However, these methods are vulnerable to external factors, such as rain and fog. Also, it is important to calibrate the camera before the measurement takes place to reduce errors for the span of interest. Hence, the generality of the method is low; that is, one has to profile the camera in different settings in different spans of the network. This makes the terrestrial methods even more labour-intensive.

2.3 | Line robot

Line robots are mobile platforms installed on the overhead line to monitor their real-time status. It can carry different sensors, including cameras and LIDAR, to measure different parameters of the overhead line, including sag, current and temperature.

In [35], a power line inspection robot was used to measure the line sagging. The robot moved along the overhead line and was remotely controlled to acquire and send sensor data. The measurement error for sag was less than 2%.

Similarly, in [36], another line recon robot was used to measure the line parameters, including temperature, current and angle of inclination, using different gyro-accelerometric sensors. It can work automatically, semi-automatically or manually. The work showed a successful application of sag calculation but did not provide any error analysis.

Remarks: Line robots are reliable and convenient. They provide good real-time monitoring, but they are expensive and hard to maintain. Their installation also requires outage access too. They could be a good choice if there is a special or important span of the overhead line whose real-time monitoring is vital. For general monitoring purposes, their deployment cost may be too high. Also, unlike the aerial and terrestrial methods discussed before that work in a non-contact way, line robots operate on the overhead line in a contact way, so that this may affect the normal operation of the power network, as the weight can increase the sagging of the line as well.

2.4 | GPS

Global positioning system (GPS) is well known for localization and ranging. It uses signals transmitted by four or more satellites to calculate the position of a ground target. For security reasons, GPS signals are deliberately inserted by the US government with some interference so that a standard measurement error is often above 30 m known as selective availability. Thus, to use GPS for sag monitoring, one often needs at least two satellite receivers to operate in a differential GPS mode to remove the selective availability error, a base on the ground with a known location and a rover on the overhead line whose sag is to be measured. Then, the two received GPS signals can be exchanged via communications equipment to reduce the calculation error.

In [37], the use of differential GPS was proposed to calculate the sag of overhead lines. One GPS receiver was installed on the line and one was installed on the ground. Both sent their received GPS signals to a control centre for processing. To obtain the 3D coordinates of the rover or the transmission line, first, time-distance equations need to be solved. Then, differential GPS correction was performed to remove the selective availability error. After that, bad data rejection was performed before a tuned filter estimation of the three coordinates. With a confidence level of 70%, the accuracy was in the range of 19.6 cm. A detailed discussion of the method can also be found in their Ph.D. thesis [38].

In [39], differential GPS was studied but focused on digital signal processing techniques to improve its accuracy over [37]. Specifically, after bad data rejection, least squares parameter estimation and Haar wavelet analysis were performed to improve the quality of the GPS data further. This improved the accuracy at 70% confidence level to 17.2 cm. Similar accuracy was also reported in [40].

In [41], the GPS method was tested in India. One GPS receiver was used but GPS measurements were taken at 2 to 3 different places to reduce error in raw GPS data. Then, signal processing was performed by using least squares parameter estimation, similar to [37]. The estimation error is about 20% of the true value or around 10 m.

In [42], the authors extended the work of [41] by adding wavelet analysis of the GPS data, similar to [39]. In this case, the accuracy of the sag calculation seemed to have improved under different conditions, varying from an error of 0.03 m for a true value of 0.8 m to an error of 0.9 m out of a true value of 0.3 m. A case study was performed by these authors in [43] in India.

In [44] and [45], a real-time sag measurement system using differential GPS was studied, where a real-time signal processing module was integrated with the GPS system. Different conditions of the overhead line current were examined using experiments. It was reported that this method has an accuracy of about 1 inch. Also, it was found that to balance the real-time

monitoring and real-time computation, the best processing window size was about 60 or 120 s using an exponential smoothing function for GPS measurements.

In [46], to tackle the high cost of GPS receivers, a cluster of cheap GPS receivers was used to replace the two expensive receivers to lower the cost. Also, Kalman filter and bad data rejection were used to reduce the measurement error from 4.5 to 0.45 and 0.37 m, respectively.

Remarks. The GPS method has a high cost in terms of both equipment and service. Hence, they can be used to monitor key spans in the power network. Moreover, compared with the aerial and terrestrial methods discussed above, their accuracy is not as high. Nevertheless, the GPS methods are not affected by weather conditions or external disturbances and they can be used in most areas without any access problems, as GPS satellites have a large coverage. Note that most of them still need installation of a GPS receiver on the overhead line and hence, it may have to work in a contact way.

2.5 | Summary

In summary, the direct methods use laser scanners, cameras or GPS receivers as sensors to measure the sag or shape of the line directly. These sensors could be expensive. The laser scanners and cameras can operate in a non-contact and non-invasive manner, but for better accuracy, markers often installed on the overhead line. The scanners and cameras can be carried by an aerial platform or a terrestrial platform or be fixed on the ground or the support tower. The line robots and the GPS receivers operate in a contact or invasive manner where a sensor must be installed on the overhead line. Thus, in addition to their expensive devices, their installation and maintenance are also at a high cost. Thus, the direct methods also incur high installation and maintenance costs. Moreover, all these methods will require sophisticated image processing or signal processing techniques in order to extract the sag profile from images or signals, and the accuracy is largely affected by the algorithms applied. Table 1 summarises the direct methods discussed.

3 | INDIRECT METHODS

Unlike the direct methods in the above section that measure the sag or the shape of the overhead line directly using cameras, laser scanners or GPS receivers, the indirect methods measure a parameter that is related to or determined by the sag and then use the mechanical, electrical or magnetic properties of the overhead line to calculate the sag from the measured parameter. The parameters commonly used include the tension, the temperature, the span length, the tilt, the magnetic flux density, the vibration frequency, the path loss, the space potential induced by the transmission line, the PMU measurements, and the power carrier signal behaviors. Next, we will discuss these indirect methods one by one for sag calculation. We will start with the most commonly used method that takes advantage of the relationship between sag and tension. Many industrial standards for sagging monitoring are based on the sag-tension formula.

3.1 | Tension

Sag is inversely proportional to the tension in the overhead line. When the tension is above a certain limit, the overhead line may break, and hence one often increases the sag to reduce the tension in the line, at the cost of increased expenditure and reduced power transfer efficiency due to a longer line. Most works on sag calculation using tension measurements are based on the catenary equation

$$y = \frac{H}{W}\left(\cosh\frac{Wx}{H} - 1\right) \tag{1}$$

where H is the horizontal component of the tension in the line, W is the weight or loading of the line, cosh(.) is the hyperbolic cosine function, x is the distance to the middle of the span and y is any position on the overhead line. The sag is calculated at the middle of the span when $x = L/2$, where L is the span length, to give

$$S = \frac{H}{W}\left(\cosh\frac{WL}{2H} - 1\right). \tag{2}$$

Also the tension at the support or the transmission tower where it is the largest is determined by

$$T = H \times \cosh\frac{WL}{2H}. \tag{3}$$

Using (2) and (3), H can be eliminated to derive a direct relationship between the sag S and the tension T. However, the hyperbolic function is not easy to calculate, especially on a simple calculator for real-time calculation. Hence, many of these works have focused on simplifying the calculation by using the parabolic approximation or series expansion. These methods are referred to as numerical methods. They are often based on single-material conductors or conventional homogeneous conductors. For composite conductors, the above equations do not apply and hence, in addition to numerical methods, graphical methods have also been developed by using the stress–strain curves. Finally, some works use hybrid methods by combining numerical and graphical methods for higher accuracy and better generality.

3.1.1 | Numerical methods

One of the earliest works on numerical methods for sag-tension calculation was by Dwight in 1926 [47], where the hyperbolic cosine function in the sag-tension formula was expanded into a Taylor series and approximations were then made by taking the first few terms of the series in the calculation. Both levelled supports and inclined supports were studied in [47]. The changes in

TABLE 1 Comparison of the direct methods for sagging monitoring.

Reference	Method	Hardware	Software	Accuracy	Contact
[9]	Aerial	UAV+camera	Decorrelation stretch, modified Prewitt filter, random sample consensus	15–30 cm	No
[10]	Aerial	Helicopter+LIDAR	Distance between line and tree	93 cm for distance	No
[11]	Aerial	Helicopter+LIDAR	Classification, local affine model	86.9% for classification, 72.1% for identification	No
[12]	Aerial	Simulation	Weather conditions, mechanical computation	65 cm	No
[13]	Aerial	UAV+rod on the line	Active vision, nonlinear least squares regression	1.269–4.423%	Yes
[14, 15]	Aerial	UAV+LIDAR	Random sample consensus, flight information	1.33%, 3–5%	No
[16]	Aerial	UAV+camera+GPS+laser	Contrast enhancement, threshold segmentation, improved Harris detection, contour fitting	0.38%	No
[17–23]	Terrestrial	Ground infrared laser system	Elevation angle and distance to the line	5 cm	No
[24]	Terrestrial	Laser scanner Leica Scan Station P30	Point cloud	0.2 cm	No
[25]	Terrestrial	Two optical sensors	Distance and angle to the line	N/A	Yes
[26]	Terrestrial	Nova OHLM	N/A	N/A	Yes
[27, 28]	Terrestrial	Camera	Background removal, contour detection	3–5%	No
[29]	Terrestrial	Two cameras + markers on the line	Displacement of the line	0.003 cm	Yes
[30, 32]	Terrestrial	Camera	Template matching	0.13 cm	No
[31]	Terrestrial	Camera + markers on the line	Direct linear transformation	1.09–29.38%	Yes
[35]	Line robot	Power line inspection robot	N/A	2%	Yes
[36]	Line robot	Line recon robot + sensors	N/A	N/A	Yes
[37, 38]	GPS	Two differential GPS receivers	Bad data rejection	19.6 cm	Yes
[39, 40]	GPS	Two differential GPS receivers	Bad data rejection, least squares estimation and Haar wavelet analysis	17.2 cm	Yes
[41]	GPS	One GPS receiver	Least squares estimation	1000 cm	Yes
[42, 43]	GPS	One GPS receiver	Least squares estimation, wavelet analysis	3–90 cm	Yes
[44, 45]	GPS	Two differential GPS receivers	Real-time signal processing	2.54 cm	Yes
[46]	GPS	More than two low-cost GPS receivers	Kalman filter, bad data rejection	37 cm–45 m	Yes

Abbreviations: GPS, global positioning system; UAV, unmanned aerial vehicles.

temperature corresponding to changes in deflection and loading were also considered in the sag calculation by calculating the expansion of the span length due to a temperature increase.

In [48], instead of using a series expansion, a Newton– Raphson method was used to iteratively solve the hyperbolic cosine function in the catenary equation for inclined spans. The temperature and loading were not considered and it only provided a numerical solution to the catenary equation.

In [49] and [50], the authors proposed a mechanical state estimation method to calculate the sag using a set of known parameters, including temperature, tension, weight, span length, slack, and so on. The parabolic approximation was used in the estimation. Similar parameters were also used in [51] to calculate the sag. In [52] and [53], by using the symmetry of level spans, only one tension sensor was used to measure the tension on one support, and then this measurement was applied with the temperature to calculate the sag to reduce the number of sensors and amount of data. The calculation method is similar to [49] and [50] by using mechanical state estimation and the parabolic approximation.

In [54], the non-linear tension state equation given in [55] was approximated using polynomials, instead of using iteration or trial-and-error, and solved to give the tension value, which was then used to calculate the sag using the sag-tension formula as

$$S = \frac{WL^2}{8H}, \tag{4}$$

where H is the horizontal tension, L is the span length and W is the weight or loading. In [56], the numerical method was applied to calculate the sag for inclined spans in hilly areas using the tension for AAAC conductors. Similar work was performed in [57] for a 330 kV transmission line supported by either levelled spans or inclined spans. In addition, the clearance to ground was also calculated.

In [58], a new method was proposed by using real-time measurements of temperature and inclination at certain point on the line to improve a non-linear mechanical model that was initially a catenary curve used to model the 3D shape of the power line. The sag value was extracted from the line shape.

3.1.2 | Graphical methods

The numerical method works for conventional homogeneous conductors but not for composite conductors, whose sag-tension relationship is more complicated. In this case, graphical methods can be used. For the graphical methods, the earliest used method was in [59], which has been implemented in many commercial software programs such as SAG10 or PLS-CADD. As discussed before, such methods use the stress–strain curves from experiments instead of the catenary equation from geometrical theories. The curves for the core and the aluminium are obtained separately to account for the composite structures of the conductors.

In [60] and [61], a graphical method called the strain summation method was proposed by summing up the measured strains, including thermal strain, slack, elastic settling and creep strain, based on which the sag at a given temperature was calculated. The graphical method relies on the stress–strain curves of the materials that make up the conductor and is usually used to calculate the sag of composite conductors.

Similarly, in [62] and [63], the authors developed graphical methods for different requirements of the gap-type conductors. These methods were also based on the strain summation method, but with some additional improvements. For example, independent core and aluminium reference lengths were assumed. Also, the calculation of the creep developed during the installation and its change was discussed in details.

3.1.3 | Hybrid methods

The numerical methods have wide applicability by using simple yet general mathematical models for the overhead line, but practical lines may deviate from these models. The graphical methods are heuristic by obtaining stress–strain curves from practical experiments but lack generality. Thus, other works have combined these two methods trying to have "the best of both."

In [64], based on the catenary equation, a hybrid method was developed by using simple arithmetical calculations from the catenary equation as well as several tables and figures for the stress–strain chart to calculate the sag for various final and initial conditions of the overhead line. The method is applicable to conductors whose modulus of elasticity and coefficient of expansion are uniform throughout the cross-section.

Ref. [65] is one of the most cited works on sag-tension calculation. In this work, based on experience from Bonneville Power Administration in US, a hybrid graphical-numerical method was developed, where the catenary equation from the numerical method for a given span length was superimposed with the tension-strain curve of a considered conductor from the graphical method for each temperature concerned. The tension-strain curves were developed using field measurements for different conductors, including ACSR.

In [66], a hybrid numerical method was proposed for composite conductors based on a modification to the numerical method to accurately calculate the sag for composite conductors that have a bilinear relationship between sag and temperature instead of the linear relationship for single-material conductors. The main algorithm still followed the numerical method as in [47] - [58] but it used the stress–strain curves of composite conductors to determine the initial load distribution between the components of the conductor for higher accuracy. Specifically, it calculated the sag as a function of the length and slack as

$$S = \sqrt{\frac{3D(l - D)}{8}}, \tag{5}$$

and then updated the length of the overhead line in the span l as a function of the thermal expansion and mechanical elongation using the stress–strain curves, where D is the slack.

In [67], the catenary equation, the stress–strain relationships from curves, the relationship between different strains, and a tension balance equation were combined into a single equation and the tension of the line in a ruling span was then determined by solving this equation approximated as a polynomial. The sag was calculated from the solved tension.

In [68] - [70], existing sag-tension calculation methods were discussed. They also recommended very detailed guidelines on how to calculate sag from tension.

3.1.4 | Factors affecting sag-tension calculations

The previous subsections cover the main methods for the calculation of sag from tension. However, a lot of factors will affect the calculation of the sag using the sag-tension relationship, in addition to the tension. For example, ice could add weight to the line to increase the sag. Temperature could vary due to wind or seasons to change the sag. These factors could have different sensitivities in the calculation of the sag using the sag-tension formula. Hence, some of the works in the literature have focused on examining the sensitivity of different factors to sag calculation.

In [71], using a parabolic approximation for sag, the sensitivity of sag to different parameters was discussed. It was found that the conductor type and the age of the line have a significant impact on sag calculation. Among the conductor thermal parameters, the wind speed, wind direction, sunlight have a significant impact, while the ambient temperature, the direction and altitude of the line, and the time of the day have negligible impact. Also, for the factors ignored by the IEEE standard in the sag calculation, the vertical wind speed has a significant impact; while the temperature distribution within the cross-section, radiation and standard deviation of wind speed have negligible impact. Also, some known thermal factors, such as an error in low wind speed measurement, variation of wind speed along the span have significant impact. Other factors from installation, design and operation could impact the sag calculation too, such as deflection, creep, temperature sensing error. In summary, the conclusion was that, if many of the sag

calculation error sources cannot be identified, it is better to be generous with the safety margins, as the use of the sag-tension relationship alone is not enough.

In [72], another work was performed to analyse the error sources of sag calculation using the sag-tension formula. It covered parameters of the conductor, such as weight, modulus of elasticity, coefficient of thermal expansion, parameters of the line section, such as the span length, the suspension tower, and weather parameters. These parameters caused uncertainties in the sag calculation. It was observed that wind speed, rain have significant impact on sag calculation. The influence of span length increases with the length. A negative error in the modulus of elasticity and a positive error in the weight lead to the largest error in tension.

In [73], the effects of the measurement errors of six parameters, span length, sag, temperature, elasticity modulus, weight per meter and conductor creep, on the sag calculation error were analysed. A formula was obtained by differentiating the state equation for the total error of sag calculation as a weighted sum of six measurement errors. It was reported that the error in elasticity modulus and the error in creep have a weak impact on the total sag error, while sag measurement error, temperature measurement error have a significant impact.

In [74], the sag was calculated by approximating the catenary curve as a squared function of $y = ax^2$ and the effects of six parameters, conductor weight, tensile strength, span length, elevation angle, temperature and wind, were discussed. Simulation showed that temperature has higher impact than wind on the sag calculation, while the impact of the elevation angle increases with the elevation angle.

In [75], the impact of temperature and wind on the sag calculation was studied. It was shown that an increase in temperature has a direct impact on sag, while an increase in wind speed has a direct impact on tension and therefore an indirect impact on sag. In [76], the impact of conductor heating due to transmission line uprating was studied by linearizing the non-linear stress-elongation equation and then calculating the sag variation due to the span length and stress changes caused by temperature change. For a given span length, there is a special conductor stress where the sag variation due to heating is the largest. Thus, conductor elastic strain variation due to heating should be considered. Also, sag variation due to heating is larger for longer span. In [77] and [78], the icing effect on sag calculation was investigated and online monitoring systems for icing were developed.

The above studies reveal that the sensitivities of different parameters in the sag calculation using the sag-tension formula are different and must be considered in order to evaluate the sources of errors for sag calculation. Thus, other researchers have tried to improve the accuracy of sag calculation by modelling these sources of errors and account them in the calculation of sag. In [79] and [80], affine arithmetic models were used to model the errors caused by ice, wind, load and weight and then applied them to the sag-tension formula in (5) for better results. For example, instead of using a single value of weight or loading W in (4), this calculation used an affine model of

$$W = W_0 + \sum_{i=1}^{m} W_i \epsilon_i \tag{6}$$

where W_i are partial derivatives of weight with respect to different parameters and ϵ_i are the errors in different parameters. In [81], probabilistic models of these factors were assumed to calculate the sag using the catenary equation.

Remarks. The sag-tension method is one of the earliest and also the most widely used method to calculate the sag from the tension. It can be calculated using the numerical method based on the catenary equation and its approximations, or the graphical method using the stress–strain curves or their combination. The numerical method is accurate and general but the overhead line must follow the mathematical models assumed. In practice, there are a lot of factors and dynamics that may make the model invalid. The graphical method comes from experiments but is then limited by the experimental conditions, such as temperatures and spans, and it does not apply to all cases. In addition to tension, many factors affect the sag calculation directly or indirectly. It is important to identify as many such factors as possible to make the calculation accurate and to give sufficient margins of error in designs. Finally, these factors may be modelled deterministically as affine arithmetic or probabilistically as random variables for better accuracy. Table 2 summarizes different tension methods for sagging monitoring.

3.2 | Temperature-current

In addition to the sag-tension relationship, the sag-temperature relationship is often used to calculate the sag as well. The temperature is actually an important parameter for sag monitoring, as thermal expansion is one of the main reasons of sagging. It is also the key parameter for dynamic line rating and is closely related to the current in the overhead line.

In [82], the authors used an existing real-time ampacity program to predict the instantaneous temperature from the current in the line and then used this temperature in an existing sag-tension program to calculate the sag. It was designed to predict temperature and sag for temperatures as high as 250°. The prediction was compared with measurements on two ACSR conductors. The accuracy of the predicted sag was found to decrease as the average conductor temperature increases. For temperatures less than 150°, nearly 70% of the time the predicted sag was within 5% of the measured value, while for temperatures greater than 150°, only 65% of the time the predicted sag was within 5% of the measured value. Compared with the graphical method for composite conductors in the tension calculation that only assumes specific temperature and location for the stress–strain curves, this method used real-time temperature. Also, this method can be applied to the new high-temperature low-sag (HTLS) conductors.

In [83], the ruling span method used for sag calculation was improved. Traditional ruling span method gives satisfactory

TABLE 2 Comparison of the tension methods for sagging monitoring.

Reference	Method	Theory	Factors considered
[47]	Numerical	Taylor series expansion	Temperature, deflection and loading
[48]	Numerical	Newton– Raphson	None
[49]–[51]	Numerical	Mechanical state estimation	Temperature, tension, weight, span length
[52, 53]	Numerical	Symmetry of span and mechanical state estimation	Temperature
[54]	Numerical	Non-linear tension state equation, polynomial approximation	Weight, span length
[56, 57]	Numerical	Tension for AAAC conductors	None
[58]	Numerical	Non-linear mechanical model	Temperature, inclination
[59]	Graphical	Stress– strain curves	None
[60, 61]	Graphical	Strain summation	Temperature
[62, 63]	Graphical	Improved strain summation	Temperature, creep
[64]	Hybrid	Catenary equation + stress– strain chart	Constant elasticity modulus and expansion coefficient
[65]	Hybrid	Catenary equation + tension– strain curve	Temperature, span length
[66]	Hybrid	Bilinear between sag and temperature + stress– strain curves	Slack, span length
[67]	Hybrid	Catenary equation+stress– strain curves + strain relationships + tension balance equation	None

Abbreviations: AAAC, aluminum alloy conductor.

accuracy for levelled lines with relatively uniform spans at any temperature or any span length of a levelled line at low temperature, but it may have large errors in a line segment with significantly unequal spans at high temperature. This new method used the rotational stiffness of suspension insulator strings to calculate sags of multi-span line segments at different temperatures using the parabolic approximation and balance of horizontal force at each conductor support. The change in span length due to temperature change was analysed.

In [84], for HTLS conductors, a holistic approach for calculating the sag at any temperature and power frequency was proposed by considering the mechanical and electrical parameters of the overall system. The calculation was performed at three different levels: mechanical, electrical and aging. Each level was fed with the overhead line structure data, such as span length, type of insulation set and heights above the ground, weather data, such as ice thickness, ice density and wind speed, conductor data, such as density, modulus of elasticity, coefficient of thermal expansion and finally the operational data, such as maximum operating temperature and system frequency during its operation. These three levels of computation were then combined to give the final conductor tension and sag with creep.

In [85] and [86], a sag monitoring system was developed for a 138 kV transmission line. An optoelectronic current transformer was used to measure the line current and a temperature sensor was used to measure the line temperature. A marker was installed in the middle of the span to measure the sag from photographs taken by a camera and use neural networks for image processing. Then these measurements were sent to a ground receiver via optical fibres to obtain the sag-current relationship and the sag-temperature relationship. Using these two relationships, temperature and current were then measured to estimate future sags.

Remarks. The temperature–current methods essentially still use the sag-tension formulas but through the parameters of temperature and current to calculate the sag more indirectly. On the other hand, the effects of the temperature and the current have also been considered in the tension method in the previous subsection. Thus, the temperature– current method and the tension method are closely related with similar performance.

3.3 | Span length

Most methods in Sections 3.1 and 3.2 calculate the sag in the middle of the span or from the straight line joining two supports to the lowest point of the span. However, it is also useful to calculate the sag as a function of any interval on the span varying from zero to the maximum and then to zero again.

In [87], the sag as a function of the length of any internal on the span was derived. Both levelled spans and inclined spans were considered. Also, both the catenary equation for long spans and the parabolic approximation for short spans were studied.

In [88], the sag was calculated as a function of the span length as

$$S = \frac{WL^2}{8\sigma\cos(\alpha)}, \tag{7}$$

where W is the loading, L is the span length, σ is the stress and α is angle of elevation. The stress was obtained by solving a cubic polynomial from the state equation of stress for overhead lines at different temperatures and loading.

Remarks. The span length methods are very similar to the numerical methods in Section 3.1, by using the parameter

of the span length instead of tension. Thus, they have similar complexity.

3.4 | Tilt

The sag is also a function of the angle of tilt of the line at the support, which can be derived from the catenary equation using the geometry of a sagged line. This can be observed from Figure 1 too. Hence, one can measure this angle and then to calculate the sag from the angle of tilt.

In [89], a dual-axis tilt sensor was installed near the support to measure the angle of tilt of the line to the ground and the swing angle simultaneously. The measurement was sent to a controller via GPRS communications link to calculate the sag. A maximum error of −0.32% was reported. Similarly, in [90], a dual-axis tilt sensor was also used to measure the slope angle or tilt angle of the line and then used these measurements to calculate the sag based on the catenary equation for inclined supports when the line swings. In the US patent [91], a similar idea was proposed by using an accelerometer sensor to measure the tilt angle based on which the sag was monitored.

In [92], the tension, temperature, tile angle and other transmission line parameters were used to calculate the sag. Unlike previous works, it considered the tilt of transmission tower due to hazards or attacks by applying a least squares state estimation method to the sag-tension formula that has been geometrically transformed to account for the tower tilt. It was shown that the increase of sag could be 55% of the non-tilted-tower case and that the proposed method had a maximum sag calculation error of 1.5% in this case.

Remarks: Similar to the tension and the span length, the tilt is just another geometrical parameter related to the sag. Thus, the sag-tilt relationship is highly relevant to the sag-tension relationship for inclined supports and with swings. This method often gives high accuracy but requires the installation of accelerometer sensors near the support towers to measure the angle of tilt.

3.5 | Air pressure

The sag is the height difference between the lowest point on the span and the support tower. Barometer can measure the height or the altitude through the change in air pressure. Hence, in [93], two barometers were used: one installed at the bottom of the span and the other on the support tower. Then their air pressures were measured to calculate the altitudes as

$$h = \frac{(T + 273.15)\left((101.325/P)^{\frac{1}{5.257}} - 1\right)}{0.0065}, \tag{8}$$

where P is the atmospheric pressure measured in kPa and T is the temperature in degrees. The sag was calculated as the difference of two altitudes. The accuracy of this method relies heavily on the precision of the barometer used.

Remarks. The air pressure method is one of the most straightforward and easiest ways to calculate the sag. However, it is a contact method, as barometer needs to be installed on the line. Its accuracy is predominantly determined by the sensitivity of the barometer used, as the sag is a very small height difference for significant air pressure change.

3.6 | Magnetic Field

The relationship between the sag and the magnetic field is probably the second widely used method for sag monitoring. When the current flows through the power line, it will generate a magnetic field around the line and the amplitude of the magnetic field depends on the intensity of the current and the distance to the overhead line. Hence, by measuring the amplitudes of the magnetic field at different positions using magnetic sensors, the sag can be calculated as the difference between distances.

Most of these methods rely on the Biot– Savart law for magnetic field, given by

$$\hat{\mathbf{B}_0} = \mu_0 \int \frac{I(l)dl \times \mathbf{a}_0(\mathbf{l})}{4\pi|\mathbf{r}_0(\mathbf{l})|^2} \tag{9}$$

where $I(l)$ is the current at the position of l in the line, $\mathbf{r}_0(\mathbf{l})$ is a position vector from the source of the magnetic field to a point in the field, and $\mathbf{a}_0(\mathbf{l})$ is a unit vector in the direction of $\mathbf{r}_0(\mathbf{l})$. Many works have assumed that the overhead line l is a straight line with infinite length. In this case, the integral can be solved to give

$$B = \frac{\mu_0 I}{2\pi r} \tag{10}$$

so that the amplitude of the magnetic field is a function of the current in the conductor I and the distance from the conductor to the observation point r, such as the ground. In [94], instead of a straight line, a more realistic catenary curve was used to solve the Biot– Savart integral. The magnetic field is still a function of the current and the distance. Hence, if one can use several sensors to measure the magnetic field at different observation points and know the values of the currents, the distances calculated from the integral can be used to estimate the sag as the difference between two heights.

One of the earliest works on this method was in [95], where three magnetic field sensors were buried underground right below the middle of the span with known locations. Then, these locations were used with the magnetic field measurements to estimate the clearance, the phase current, the ampacity as well as sag. Since the measurement was non-contact, no power cut or field personnel were required. This became a patent in [96].

Similarly, in [97], the authors used magnetoresistive sensors to measure the emanated magnetic field from the line at various locations on the ground and then calculated the source position and current to estimate the sag. Again the method is

non-contact with simple installation and without power cut. It was then tested on a 500 kV transmission line. The error was around 0.246%. It used two sensors. This method was extended in [98] to measure more parameters. In this work, the magnetic field distribution at the ground level was sampled at various locations for transmission lines operating with sagging, galloping and current imbalance. The relationships between magnetic field variations and different operation states of the line were obtained, based on which a source reconstruction was performed to reconstruct the spatial and electrical parameters of the line based on the magnetic field distribution. This was then tested on 500 and 220 kV transmission lines. The error was less than 0.2%.

In [99]–[101], a uniaxial magnetic sensor was installed at the support tower to measure the magnetic field and an electrical sensor was used at the substation to measure the phase current. The relationship between the variation of sag and the variation of the magnetic field was observed for the same current. This relationship was then simulated and compared with measured magnetic fields to estimate the change due to sag. The error was less than 1%. Moreover, in [101], an array of magnetic sensors was used and their optimal locations were studied, as the magnetic flux density and therefore the sag was sensitive to the location of the sensor.

In [102], ground magnetoresistive sensor was used to measure the magnetic flux density along the centre line from the three-phase transmission lines to estimate the support tower inclination, the transmission line sag and the transmission current simultaneously. An algorithm based on artificial immune system was applied to estimate the sag and the tower tilt angle and reconstruct the current. The error of sag calculation was less than 0.3%. An array of five dual-axis magnetic sensors was used.

In [103], two magnetic field sensors were combined into one probe to measure the magnetic field at different distances to the line, based on which the positioning of the line and the current in the line were calculated. Some special signal processing was applied when the current was low and the magnetic field was weak. The average error for distance calculation was about 1%.

In [104, 105], the magnetic flux density was again used to calculate the sag of the conductor. However, instead of using the catenary curve in the Biot– Savart integral, the authors proposed to use a tilted straight line model to approximate the catenary curve for simple and real-time calculation of sag. The model was then calibrated by tuning the model coefficients to match flux density vectors in the real catenary curve for enhanced accuracy. The sag can be calculated using the y component of the measurement with an error of less than 2%.

Remarks. The magnetic field method provides very accurate estimation of the sag. It can also be non-contact, without any installation on the line or on the tower (although some works do require sensors installed on the tower, they can alternatively be placed on the ground). This makes its use simple. On the other hand, accurate estimation of sag often requires several sensors and the placement of sensors also determine the accuracy so that the choices of locations are important.

3.7 | RF

The path loss in radio frequency communications depends on the distance between the transmitter and the receiver, as the strength of the radio signal attenuates when the distance increases. Hence, if one knows the received signal strength and the transmitted signal strength, the distance may be calculated. In the case of sag calculation, if the transmitter is in the middle of the span of an overhead line and the receiver is on the ground, the sag may be estimated using these distances from the received signal strengths.

In [106], the authors used the millimetre wave radio signal to measure the distance between the line and the ground to estimate the sag. Specifically, a single transmitter was placed on the line to transmit millimetre wave signals to a receiver on the ground. The path loss was calculated from the received signal power and then the sag was calculated using the averaged distance. The error of sag was quite large, 6.6%, 9.3% and 12.9% for a distance of 5 m, 10 m and 15 m, respectively. To improve the accuracy, a further work was conducted in [107], where in addition to a transmitter on the line, both a receiver and an angle-of-arrival sensor were placed on the support tower to measure not only the received signal power but also the angle of its arrival. The sag was then calculated using the distance from the path loss in the received signal power and the angle of arrival. The calculation was very sensitive to the angle of arrival error. When the angle can be measured accurately, the error of sag was less than 4% in most cases considered. More details of this method can be found in [108] and [109] by the same authors.

In [110], instead of using the millimetre wave signals, radio frequency identification (RFID) technique was used, where an RFID tag was placed on the line and a reader acting as a passive radar was placed on the ground to measure the received signal power and angle of arrival from the tag. A more detailed discussion can be found in their thesis [111].

In [112] and [113], an Internet-of-Things based sag monitoring system was proposed, where the sag sensor contains a tri-axial accelerometer installed on the line to measure the angle between the gravity and the z-direction, which was used to calculate the sag based on the catenary equation. Then this was sent using the ZigBee protocol wirelessly to the remote controller. This method actually used something similar to tilt to measure the sag but then transmitted the sag value using radio waves. Finally, in [114], the authors compared different wireless communications techniques to transmit measurements from the line to the ground remote controller, as the radio signals would be interfered by the electromagnetic field generated by the transmission line and this interference has different impact on different wireless techniques.

Remarks. The RF method in principle is similar to laser scan, as laser is a type of optical wave too, except that the radio wave has much larger wavelength and therefore lower resolution than the optical wave. Nevertheless, wireless communications is moving from microwave to millimetre wave to future terahertz wave so that their wavelength is getting smaller and smaller for better resolution. In the future, this method can

become more accurate by calculating the sag from the distance. Also, radio communications is important for data transmission from sensors to ground controllers. This requires further investigation too.

3.8 | Vibration

Due to the wind and actions of other external and internal loads on the line, the line span between two support towers can swing like a pendulum, where the conductor acts as the body rotating around the straight line between two support towers. In this case, the sag is the radius of the swing around the straight line. Hence, one can measure the period or frequency of the vibration or swing of the line to obtain the sag.

In [115], the authors treated the conductor as a physical pendulum around the straight line between the two support towers and derived the relationship between the sag and the period of swing as

$$S = 0.31T^2 \tag{11}$$

where T is the period of the swing or the oscillation period. Thus, the sag can be calculated by measuring the natural harmonic vibration of the conductor hanging in a span with supports at the same heights. An inclinometer was used to measure the period then. This method turned out to be very accurate with an error of less than 0.85% in the considered setting. A more detailed discussion was provided in [116], considering different cases of swing, with reduced errors of less than 0.1%.

In [117], instead of inclinometer on the line, the authors installed markers on the line and then used high-speed digital cameras to capture the motion of the markers in the video sequence, based on which the vibration was measured and the clearance to ground was calculated.

In [118], the authors reported works by two system operators in Europe on their Ampacimon system that measured the sag of an overhead line in real time by measuring the conductor vibrations using accelerometers. The conductor sag was then calculated based on these measurements using data processing (fast Fourier transform) and simple mathematical equations. No details on the calculation were revealed in the work but the fast Fourier transform should be used to extract the vibration frequency from accelerometer measurements for sag calculation. More technical details were provided in [119]. In this work, using the catenary equation and the dynamics of the line, the relationship between the sag and the vibration frequency was obtained as

$$S = \frac{W}{32f_0^2} \tag{12}$$

where W is the loading of the line as defined before and f_0 is the frequency of vibration. The work reported an error of sag calculation within 2%.

Remarks. The vibration method has nicely utilized the relationship between sag and vibration period/frequency to give very accurate sag calculation. The relationship between the vibration frequency or period and the sag is also very simple that only requires the parameter of the loading or a constant. However, this simplicity is achieved at the cost of lack of generality. For example, different temperatures will lead to different frequencies etc. leading to different constants. Hence, this method has to be re-tuned every time the conditions or span change. Another disadvantage is that its accuracy becomes low when the vibration is small or the line does not swing at all.

3.9 | Space potential

In addition to the magnetic field, the current in the overhead line also generates an electrical field, which can be used for non-contact measurement of sag as well, similar to the magnetic flux density method discussed previously. In this case, the electrical property of the overhead line is used. The principle of all these methods is to first solve the electromagnetic field distribution of the transmission line, then establish the relationship between the field source parameter and the spatial electromagnetic field distribution value, and finally inversely calculate the field source parameter by collecting the electromagnetic field distribution values collected at various points in space during the operation of the overhead line.

In [120], inspired by the magnetic field method, the authors proposed the use of space potential in the electrical field to measure the amplitude and relative phase of the transmission line's space potential in two or more selected locations in the space. It measured the sum of currents induced on space potential probes placed at strategic locations near a transmission line such that the sum of currents was zero for some critical condition of the transmission line to make the measurement extremely sensitive to small changes from this condition, such as a small change in sag. The space potential was determined by the voltage of the line as well as the geometry of the line so that the sag will affect the shape of the line and therefore the space potential. A passive phase shifter was also used to enhance sensitivity.

Similarly, in [121], an electrostatic coupling model between the transmission line and the measuring locations was established and the sag was calculated from potential measurements using a potential measurement array. In this case, the space potential describing the field distribution was used to calculate the field source locations related to sag. In [122], the effects of span configuration and the conductor sag on the electric field distribution were studied for a 3D model and then these relationships and probes of electric field were used to calculate the sag.

In [123] and [124], the current induced in a grounded resistive wire due to quasi-static space potential of the transmission line was used to calculate the sag, as the potential was determined by the line geometry including the sag. This method works well for delta configured transmission lines but not so well for the more common horizontal lines.

Remarks. Both the electrical field method in this subsection and the magnetic field method in Section 3.6 give non-contact ways of measuring the sag via space potential or magnetic flux density, respectively. In some spans, this is important because the span may be too important to shut down or be blocked for access. However, both methods are quite sensitive to the locations chosen and their accuracy could be low if they are not set up properly. Also, the electromagnetic field may be more complicated than assumed, as interference may occur.

3.10 | PMU

Phasor measurement units (PMUs) take current, voltage and frequency readings in the power network and time stamp them using GPS before sending them to the control centres for planning and operation purposes. They are one of the most important measurements in the power network. These measurements can be used to calculate the sag indirectly as well.

In [125], the line admittance and impedance were calculated from the current and voltage measurements in PMUs. The average line temperature was then calculated as a function of the line resistance from the real part of the line impedance. After that, the line length was calculated from the temperature using the thermal expansion coefficient. Finally, the sag of the line was calculated from the line length and the span length using the sag-tension formula as in (5).

Similarly, in [126] and [127], the least squares method was used to estimate the line resistance and the line temperature from a series of PMU measurements. Then the sag was calculated from the line length due to the thermal expansion and the span length as in (5).

Remarks. The PMU method is convenient as the PMU measurements are often available in the network without the need for any extra sensors or their installation. Its calculation essentially depends on the sag-tension relationship using the parabolic approximation by considering the thermal heating effect. Thus, it has similar limitations and advantages as the tension method.

3.11 | Carrier signal

The sag is part of the line geometry. The change of sag leads to changes in the line geometry, which will not only change the electrical and magnetic fields near the transmission line but also change the power line carrier signal inside the transmission line. Thus, by measuring the variation of the power line carrier signal between two stations, the sag may be calculated.

In [128], a power line carrier hybrid coupler was used to inject multi-frequency continuous-wave monitoring signals in the band from 50 to 500 kHz into the transmission line. Based on the theory of natural modes for multi-conductor transmission lines, the monitoring tones were appropriately chosen at unallocated PLC frequencies to avoid interference to the normal operation of power line carrier systems. During the transmission over the multi-conductor overhead line, the tones of the signal was decomposed into natural modes which propagated at different velocities and attenuation factors to the remote PLC station. They were decoupled using an additional hybrid coupler there and the decoupled signal was analysed in the frequency domain to extract information on the physical height of the overhead conductor and therefore calculate the sag as the height change. The amplitude of the carrier signal was found to be highly correlated to the average height measured, up to 99% correlation or an error of 1%. More detailed discussion of this method can be found in their Ph.D. thesis [129].

Remarks. This method was tested and used by the transmission operator in South Africa. It uses the relationship between the amplitude of the power line carrier signal and the variation in the height of the line. It has good accuracy. The theory is simple but it requires a power line carrier signalling system with two stations. Not only the set-up is complicated but also the maintenance cost is high.

3.12 | Optical

The sag and the tension not only change the transmission line electromagnetically but also optically. Hence, optical sensors could be used to measure the optical changes caused by sag and then use their relationships to calculate the sag. Moreover, optical sensors are not sensitive to the electromagnetic field generated by the transmission line and hence, unlike the RF, magnetic field or space potential methods, they are immune to electromagnetic interference.

In [130] and [131], the chirped fibre Bragg grating sensor was used on an ACSR conductor to measure its strain, from which the sag was calculated. If one can select the chirped fiber Bragg grating transducer and the optical parameters of such a sensor appropriately, high sensitivity to the line elongation can be achieved and hence high accuracy for sag, while reducing the sensitivity to the temperature. Similar work was also conducted in [132] using fibre Bragg grating sensor.

For the photoelectric composite conductors, such as optical fibre composite overhead ground wire, it is possible to apply distributed optical fibre sensors (DOFS) to the transmission line status monitoring. Ref. [133] used a phase sensitive optical time domain reflectometry sensor to measure the phase change in the optical fibre part of the conductor caused by the sag of the line and then used these phase changes to calculate the sag as

$$S = \sqrt{\frac{3\lambda L}{32\pi n}\Delta\theta + S_0^2} \tag{13}$$

where $\Delta\theta$ is the phase change or difference, S_0 is the initial sag before the change, L is the span length, n is the refractive index of the optical fibre core and λ is the wavelength of the optical signal. The calculation error was less than 5.8% on the centimetre scale. In [134], an international patent was filed

to couple an optical fibre with the transmission line and then use a strain sensor to transmit an optical signal in the fibre and use the backscattered optical signal to measure the strain of the transmission line. Using the measured strain, the sag value was calculated using the sag-strain relationship. The shape of the line was also determined.

Remarks. The optical method uses optical sensors to measure the changes in the optical signals coupled with the transmission lines and caused by the sag to calculate the sag. It is free from electromagnetic interference and can be tuned to make the optical parameters sensitive to the change in the sag for highly accurate sag calculation. However, it requires extra optical sensors as well as extra optical fibres installed. Some method only works for certain conductors.

3.13 | Summary

In summary, the indirect methods rely on the relationships between the sag and different mechanical, thermal, electrical or magnetic parameters of the overhead line. Among them, the tension method, the temperature– current method, the span length method, the tilt method are the simplest by using the sag-tension formula. However, one has to be careful in this case, as the sag-tension formula has made a lot of simplifications and assumptions, sometimes ignoring important factors or uncertainties. The magnetic field method, the space potential method and the optical method rely on the electromagnetic or optical fields generated by the transmission line. For accurate calculation, a large number of sensors are often required. But they do give very high accuracy. Finally, the air pressure method is very simple but needs high-precision barometers. The RF method, the vibration method, the PMU method and the carrier signal method take advantage of the geometrical property of the overhead line. Their performances vary a lot, depending on the set-up. Table 3 summarizes the indirect methods discussed, excluding the tension method that mainly focus on theories rather than monitor designs.

4 | SAG PREDICTION

The methods discussed in Sections 2 and 3 mainly focus on the estimation of sag that is, acquisition of the current value of line sag. However, sag changes dynamically with time and location in practice. For more efficient network planning and control, it may be useful to predict the value of sag in the future. There are very few works on sag prediction. In this section, various sag prediction methods in the literature will be discussed.

In [135], using the line design, the conductor temperature, the loading history, wind speed and direction, and ice load, the sag of the line was predicted using a computer program developed by Ontario Hydro for the Canadian Electrical Association. The prediction used 13 thermalcouples on the line to get the temperature readings, a sag and tension device to measure the current sag and a local weather station to get the current weather conditions. The predicted sag was within 5% of the measured sag.

In [136], a tension sensor was installed between the dead-end insulator and dead-end structure. The sag was then calculated using the measured tension. The singular value decomposition chaotic method in chaos theory was applied to the time series of sag to predict the sag value in the near future. The prediction error was less than 6%.

In [137], the authors used the tensions and the current temperature, along with loading parameters and the span length to predict the temperature in the future minutes and then used the predicted temperature and the sag-temperature relationship to calculate the sag in the future. The experiment results showed the method can predict the sag in the upcoming 15 min with high reliability and for the upcoming hour with a 96% confidence level.

In [138], the sag measurements from laser scan were used to predict future sag using the support vector machine algorithm, whose parameters were optimized using the particle swarm optimization. The prediction error was at a maximum of around 7.8% without particle swarm optimization but 4.5% with particle swarm optimization.

Sag prediction is still a research area at its infancy in overhead line sagging monitoring. The methods used in the current works are not very reliable with considerable errors. However, sag values are relatively stable and there should be better ways to predict them by using advanced time series processing techniques.

Finally, for a review of some widely used sag calculation and sag prediction methods in the literature, one can refer to [139] - [142]. Note that, although [139] also provides an overview of overhead line sag monitoring methods, there is significant difference between our work and [139]. Firstly, our coverage is much wider. For example, the sag prediction method was largely ignored in [139], while this method is important for timely planning of the power network and hence, it has been discussed in detail here. Also, the graphical method and the hybrid method in sag-tension calculation were not discussed in [139], while they play crucial roles in the overhead line installation practice and have been discussed here. Secondly, our discussion is much deeper. For example, in the direct methods, this work has investigated 26 works that use different aerial or terrestrial systems to measure the sag directly (references [9] - [34]), while [139] only discussed five of them briefly. Even for the GPS method that received great attention in [139], only six works were discussed there while our work has covered ten works (references [37] - [46]). Thirdly, in addition to these coverage and discussion, our work has also offered detailed comparison of different methods in terms of hardware, software and quantitative accuracy in Tables 1–3, which are missing in [139]. These tables will allow power system designers to easily identify which methods can fit their purposes. Finally, this work has outlined research challenges in overhead line sag monitoring from different perspectives. Ref. [139] focused mainly on the wireless communications issue in sag monitoring, while this work focuses on learning, modelling and deployment issues.

TABLE 3 Comparison of the indirect methods for sagging monitoring (excluding tension).

Reference	Method	Hardware	Software	Accuracy	Contact
[82]	Temperature– current	Real-time ampacity for ACSR, HTLS conductors	Sag-tension program	5%	Yes
[83]	Temperature– current	Ruling span	Parabolic approximation, balance of horizontal forces	2%	Yes
[84]	Temperature– current	HTLS conductor	Structure data, weather data, conductor data, operational data at mechanical, electrical and aging	1–20 cm	Yes
[85, 86]	Temperature– current	Optoelectronic current transformer+temperature sensor + marker on the line + camera	Neural networks	N/A	Yes
[87]	Span length	Levelled and inclined spans	Catenary equation and parabolic approximation	N/A	Yes
[88]	Span length	N/A	State equation of stress	N/A	Yes
[89]	Tilt	Dual-axis tilt sensor	Angle of tilt, swing angle	−0.32%	Yes
[90, 91]	Tilt	Dual-axis tilt sensor or accelerometer sensor	Slope angle and tilt angle	N/A	Yes
[92]	Tilt	Accelerometer sensor	Least squares state estimation, sag-tension	1.5%	Yes
[93]	Air pressure	Two barometers	Altitude-atmospheric pressure relationship	N/A	Yes
[95, 96]	Magnetic field	Three magnetic field sensors	Biot– Savart integral	2 cm	No
[97]	Magnetic field	Magnetoresistive sensors	Biot– Savart integral	0.246%	No
[98]	Magnetic field	Magnetoresistive sensors	Source reconstruction	0.2%	No
[99]–[101]	Magnetic field	Magnetic sensor at support + electrical sensor at substation	Magnetic field-sag relationship	1%	Yes
[102]	Magnetic field	Five magnetoresistive sensors	Artificial immune system	0.3%	No
[103]	Magnetic field	Two magnetic field sensors	Magnetic field-positioning-current relationship	1%	No
[104, 105]	Magnetic field	Magnetic field sensors	Tilted straight line model for Biot– Savart integral	2%	No
[106]	RF	mmWave transmitter and receiver	Path loss	6.6–12.9%	Yes
[107]–[109]	RF	mmWave transmitter and receiver + angle-of-arrival sensor	Path loss, angle of arrival	4%	Yes
[110, 111]	RF	RFID on the line + tag reader on the ground	Received signal power, angle of arrival	N/A	Yes
[112, 113]	RF	IoT + tri-axial accelerometer on the line	ZigBee	<3.14%	Yes
[115, 116]	Vibration	Inclinometer	Swing period-sag relationship	0.1–0.85%	Yes
[117]	Vibration	Camera + markers on the line	Swing period-sag relationship	N/A	Yes
[118, 119]	Vibration	Accelerometers	Fourier transform, vibration frequency-sag relationship	2%	Yes
[120]	Space potential	Single and differential space potential probes	Potential-voltage-sag relationship	N/A	No
[121]	Space potential	Potential measurement array	Electrostatic coupling model	0–4.13%	No
[122, 123]	Space potential	Electric field probes	3D model, electric field distribution-span configuration-sag relationship	N/A	No
[124]	Space potential	Grounded resistive wire + delta configured line	Potential-line geometry relationship	2%	No
[125]	PMU	PMU device	Line admittance and impedance, line temperature, line length	N/A	Yes
[126, 127]	PMU	PMU device	Line resistance, line temperature, least squares	0.03–0.3 ft	Yes
[128, 129]	Carrier signal	Power line carrier hybrid coupler	Power line propagation theory, mode decomposition	1%	Yes
[130]–[132]	Optical	Chirped fibre Bragg grating sensor + ACSR conductor	Sag-optical parameters relationship	5–15%	Yes
[133]	Optical	Phase sensitive optical time domain reflectometry sensor	Sag-phase change relationship	5.8%	Yes
[134]	Optical	Optical fibre coupler + strain sensor	Sag-strain relationship	N/A	Yes

Abbreviations: ACSR, aluminum conductor-steel reinforced; HTLS, high temperature low sag; PMU, Phasor measurement units; RF, radio frequency; RFID, radio frequency identification.

5 | DEVICES AND INDUSTRIAL STANDARDS

Sag monitoring has been an important part of asset condition monitoring in the transmission networks for many years. Several companies and organizations have developed sag monitoring devices in the market for such applications.

One of the earliest such devices is the video sagometer developed by the Electric Power Research Institute (EPRI) [143]. This device uses cameras to capture the image of a marker located on the line and different sensors to measure wind speed, temperature and solar irradiance, based on which sag is calculated. The New York Power Authority used sagometer on their 230 kV transmission lines to show a 30–40% improvement compared with static line rating.

Another device is the overhead transmission line monitor (OTLM) developed by C&G Ljubljana. It contains several sensors to measure the temperature, wind speed, inclination, current and humidity. These are then used in the sag-tension relationship to calculate the sag for monitoring. These sensors are installed on the line but can transmit measurements to the ground via cellular, LoRA, WiFi or satellite with GPS time stamps. OTLM was used in the 110 kV transmission lines in Slovenia.

Ampacimon is another device developed for ampacity monitoring in dynamic line rating, including sag monitoring. It uses the vibration of the line to compute the sag, as discussed before in [118]. This has been used in Belgium and France in their transmission networks for ampacity improvement.

In addition to the above, Power Donut is an online dynamic rating monitoring system, including sag monitoring, that has been widely used by several companies [144] - [146]. Power Line Systems Inc. in the US developed a device called SAGSEC back in 1997 to monitor sag with multi-span tension section [147]. Also, CAT-1 and sagmeter have been developed for sag monitoring only [148, 149].

Despite the difference of networks in different countries, several industrial standards for sag monitoring have also been established. The IEEE Standard 524-2016 gives guidelines for the installation of overhead transmission line conductors. Specifically, it defines ways of creating sags in the overhead line to meet the tension and safety requirements of the conductors. It gives three methods in the standard for creating the sag: transit method, stopwatch method and dynamometer method. The transit method uses calculated angle of sight, horizontal line of sight and target. The stopwatch method measures the time taken by the reflected wave to reach the jerking point. The dynamometer method measures the tension when inserted in the same line where the sag is measured. The stopwatch and dynamometer methods are more suitable for short spans, while the transit method is for both short and long spans [150].

CIGRE Taskforce B2.12.3 developed technical report on sag-tension calculation in 2007 and then updated it in 2016. It summarizes the sag-tension method used in Section 3.1 with details on the mathematical models used. For example, it discussed both the catenary equation and its parabolic approximation, the ruling span method, elongation models for different types of conductors and the effects of different parameters on the conductor sag [69].

In addition to the IEEE and CIGRE guidelines, there are also transmission line design manuals developed by different operators in different countries.

6 | RESEARCH CHALLENGES

Although a lot of works have been conducted on overhead line sag monitoring with many methods available in the literature, especially the indirect methods, several challenges remain in order to have low-cost high-accuracy real-time monitors for overhead line sag. In the following, some of these challenges will be outlined.

6.1 | Machine learning

The accuracy of the direct method relies largely on the image processing algorithms applied. These methods do not assume any theoretical or heuristic models for the sag and therefore their accuracy is not restricted by the models. Thus, they can be applied to any spans in any networks. However, the images or video sequences captured from the laser scans, line robots or cameras need careful processing and/or pre-processing. The final accuracy depends on how good such processing is. Thus, some direct methods have errors as large as 14% while others have errors as small as 0.38%. To reduce errors, one has to either increase the complexity of the software for better processing or increase the complexity of the hardware for better equipment. Since the direct methods have already had high hardware cost, software improvement will be a better option for this purpose. In this case, machine leaning and deep learning algorithms should be used. These learning methods are well known for their high accuracy in image processing. Thus, it is a future challenge to apply more machine learning algorithms to process images and videos in the direct methods for enhanced accuracy. Also, the main application of machine learning is prediction or function approximation. Thus, another future challenge is to apply better machine learning algorithms to approximate the functional relationships between sag and other parameters in the indirect methods for higher accuracy or to replace the sag-temperature relationship and chaos theory used in [135] - [137] with machine learning algorithms to predict sag using measurements directly. For example, convolutional neural networks could be used to extract the sag information from the 3D point cloud data captured by LIDAR or 2D images captured by camera instead of using filtering and fitting. Model-based deep learning can improve accuracy by combining deep learning methods with catenary models of the overhead line. Recurrent neural networks or long-short term memory methods could be used to predict sag. Generative adversarial networks could be used to synthesize samples to make up the limited flight time in aerial systems for better training. As well, learning-based

methods could be used to replace the deterministic relationship between sag and line parameters currently adopted in the indirect methods for better accuracy. For example, it was discussed in Section 3.1 that the accuracy of the sag-tension method could be affected by many factors that have been ignored in the formula, such as ice and wind. This problem could be addressed by using an online machine learning algorithm to approximate the relationship between sag and tension directly. The parameters of the machine learning models will be trained to adapt to the ice and wind conditions for high accuracy.

6.2 | Overhead line modelling

The indirect methods require models for the sag, such as the sag-tension model, sag-temperature, the Biot– Savart law etc. Hence, the accuracy of these methods relies largely on the accuracy of these models. For example, if the line curve does not follow the catenary equation any more due to unevenly distributed icing or wind, many indirect methods may have poor accuracy or even collapse. The RF method may suffer from the inaccurate path loss model and interference from the electromagnetic field generated by the transmission line. The temperature– current method may suffer from non-uniformly distributed temperature on the conductor and inside the conductor. The PMU method may suffer from the limited availability of PMU in the network. Hence, for better accuracy, it is a future challenge to model the transmission line as accurately as possible in the indirect methods. For example, channel modelling should be performed to obtain more realistic relationship between the distance and the received signal for the RF method, more temperature sensors should be used to take temperature readings across the span in the temperature– current method, and more PMUs should be used to measure phases more locally or even for a specific span in the PMU method. Also, new probabilistic and deterministic models for errors in sag-tension calculation should be established. These models will treat temperature, current, tension and other parameters that affect the sag as random variables or Markov processes to more accurately describe sag in a hybrid stochastic-deterministic model. Also, in the Biot– Savart law and space potential methods, finite element analysis could be used to calculate the electromagnetic field without assuming the catenary equation. In the RF method, geometry-based stochastic models could be used, as they are more accurate than deterministic methods by making scatters random to cover more scenarios.

6.3 | Wide deployment

The direct methods are generally expensive or at least more expensive than the indirect methods. Thus, they are not suitable for large-scale deployment. For the indirect methods, their cost relies on the cost of individual sensors and the number of sensors used. However, most of these methods are designed for individual spans. In a power grid, there is a huge number of spans. Even a cheap monitor could incur high cost if the whole network needs to be monitored. Thus, to significantly reduce the deployment cost for large-scale monitoring, a paradigm shift in overhead line sagging monitoring design is required. For example, a camera should capture images of multiple spans at the same time for processing. Differential methods in electromagnetic fields near the transmission line should be developed to focus on the change of sag across spans so that the sag in the neighbouring spans can be calculated from the current span. It is a future challenge to develop sagging monitoring methods suitable for large-scale deployment. This will be enabled with the development of technologies in other areas. For example, as hardware technology advances, the cost of each sensor in the aforementioned methods may decrease to facilitate large-scale deployment. As cellular systems evolve towards the sixth-generation, hybrid satellite-terrestrial networks and integrated sensing and communications can be implemented to monitor the sag at large scale. Also, energy harvesting and wireless power will allow the prolonged operation of a massive number of low-power sensors.

6.4 | More new methods

Although there have been many methods on overhead line sag monitoring, more new methods could be developed. The methods presented in the literature have their own advantages and disadvantages. These methods could be mixed and matched to combine their advantages while avoiding their disadvantages. For example, the disadvantage of the magnetic field method is the large number of sensors required to sample the magnetic field, while it has high accuracy. They can be combined with the space potential method by designing sensors that can measure the magnetic field and the electric field at the same time so that less sensors are needed. Also, the direct method can be combined with the magnetic field method so that the line shape can be extracted from images and then used in the magnetic field method for sag calculation. Also, UAVs can play a more important role with on-board processing. Finally, state-of-art wireless communications provide radio coverage in a large area, which can be used to monitor line sagging via radio sensing. The key idea is to combine different existing methods in such a way that their advantages can be utilized while their disadvantages can be circumvented. Also, exploration of the relationships between sag and new physical, electrical, mechanical and electromagnetic parameters will lead to new methods.

7 | CONCLUSIONS

In this paper, different methods for overhead line sagging monitoring have been reviewed. Sag prediction methods have also been discussed. Some widely used monitoring devices with relevant industry standards have been outlined and future research challenges have been discussed. The survey reveals the following conclusions.

In terms of accuracy, the direct methods generally have high accuracy. Among the indirect methods, the magnetic field and

space potential methods (both use electromagnetic field), the tension, tilt, span length methods (all use sag-tension formula), the vibration method and the optical method have good accuracies. They are followed by the RF method, the carrier signal method, the current/temperature method, and the PMU and air pressure methods.

In terms of cost, the direct methods are generally of high cost. The use of aerial platforms, such as UAVs and helicopters, leads to huge operational costs for maintenance, personnel, fuel and so on. The use of terrestrial platforms, such as vehicles or humans, incurs large labour costs. The use of cameras, GPS and line robots also requires costly equipment. Hence, direct methods should only be used for a limited number of important spans, such as crossings. For the indirect methods, the magnetic field sensor, the space potential probe, the RF transceivers have low cost. However, these methods often require multiple sensors for high accuracy. The tension tensor, temperature tensor, current transformer, inclinometer, accelerometer and high-precision barometer cost more but these methods have good accuracy by using only one or two such sensors so that the total cost may still be reasonable. Finally, for the PMU method, carrier signal method and optical method, their sensors are more expensive. Hence, from the cost's point of view, magnetic field and space potential methods should be used, followed by the tension, tilt, span length, temperature– current, vibration and air-pressure methods.

Another issue is installation. Among the direct methods, the aerial and terrestrial methods in general only use laser or camera to remotely capture the line in a non-contact way. The GPS and line robot methods will need installation of markers, GPS receivers or robots on the overhead line and/or support towers. Among the indirect methods, the magnetic field and the space potential methods can measure the electromagnetic field on the ground. Hence, these methods are non-contact and do not need the installation of any sensors on the overhead line or their support towers. Other indirect methods, such as tension, vibration, PMU and optical, will require installation of sensors on the overhead line and/or support towers. For the non-contact methods, their installation does not require any power outage and their maintenance is also simple. Thus, they should be used in scenarios when land access is a problem for installation or when the power network operation and safety will be adversely affected by over-the-line sensors.

Finally, the generality of the method is also important. Some methods may need different settings and calibrations for different spans or conditions. This will restrict their use and deployment, as one has to customize their software and/or hardware to different uses or scenarios, while it may be preferable to use the same software and hardware for all cases without any further calibration for wide deployment. The direct method has high generality of being applied to any spans and any scenarios, weather permitting. Thus, they have high generality. Among the indirect methods, the magnetic field, space potential, RF and air pressure methods have higher generality, while the tension, temperature– current, span length, tilt, vibration, PMU, carrier signal and optical methods have lower generality. For example, the vibration method only works when the line swings. The tension, temperature– current, span length and tilt methods need to be adapted for different conductors or weather conditions. Thus, the magnetic field, space potential, RF and air pressure methods should be used for generality. Table 4 summarizes their comparison.

TABLE 4 Summary of different methods (H, High; M, Medium; L, Low).

Methods	Accuracy	Cost	Installation	Generality
Aerial	L	H	L	H
Terrestrial	L– M	H	L	H
Line robot	H	H	H	H
GPS	L	H	H	H
Tension	H	M	H	L
Temperature–current	L	M	H	L
Span length	H	M	H	L
Tilt	H	M	H	L
Air pressure	L	M	H	M
Magnetic field	H	L	L	M
RF	L	L	H	M
Vibration	H	M	H	L
Space potential	H	L	L	M
PMU	L	H	H	L
Carrier signal	L	H	H	L
Optical	H	H	H	L

Abbreviations: GPS, global positioning system; PMU, phasor measurement unit; RF, radio frequency.

AUTHOR CONTRIBUTIONS

Yunfei Chen contributes to the conceptualization and original draft preparation. Xiaolin Ding contributes to analysis, review & editing.

ACKNOWLEDGMENTS

This work was supported in part by National Grid Network Innovation Allowance under grant NIA2_NGET0013.

CONFLICT OF INTEREST STATEMENT

The authors declare no conflict of interest.

DATA AVAILABILITY STATEMENT

Data sharing not applicable to this article as no datasets were generated or analysed during the current study.

ORCID

Yunfei Chen https://orcid.org/0000-0001-8083-1805

REFERENCES

1. Omer, A.M.: Energy, environment and sustainable development. Renewable Sustainable Energy Rev. 12(9), 2265–2300 (2008)
2. https://en.wikipedia.org/wiki/Northeast_blackout_of_2003
3. Bedialauneta, M.T., Fernandez, E., Albizu, I., et al.: Factors that affect the sag-tension model of an overhead conductor. In: 2013 IEEE Grenoble Conference, pp. 1–6. IEEE, Piscataway, NJ (2013)

4. Adams, H.W.: Steel supported aluminum conductors (SSAC) for overhead transmission lines. IEEE Trans. Power App. Syst. 93(5), 1700–1705 (1974)
5. US Department of Energy, Dynamic Line Rating Report to Congress. https://www.energy.gov/sites/default/files/2021/03/f83/DLR%20Report%20-%20June%202019%20final%20-%20FOR%20PUBLIC%20USE.pdf
6. IEEE, 738-1993 - IEEE Standard for Calculating the Current-Temperature of Bare Overhead Conductors (1993). https://doi.org/10.1109/IEEESTD.1993.120365
7. CIGRE WG 22.12, The thermal behaviour of overhead line conductors. Electra 114(3), 107–25 (1992).
8. IEC: Standard TR 1597 Overhead Electrical Conductors - Calculation Methods for Stranded Bare Conductors. (1985).
9. Pastucha, E., Puniach, E., Scislowicz, A., et al.: 3D reconstruction of power lines using UAV images to monitor corridor clearance. Remote Sens. 12(22), 3698 (2020)
10. Ashidate, S-I., Murashima, S., Fujii, N.: Development of a helicopter-mounted eye-safe laser radar system for distance measurement between power transmission lines and nearby trees. IEEE Trans. Power Deliv. 17(2), 644–648 (2002)
11. McLaughlin, R.A.: Extracting transmission lines from airborne LIDAR data. IEEE Geosci. Remote. Sens. Lett. 3(2), 222–226 (2006)
12. Zhang, S.C., Liu, J.Z., Niu, Z., et al.: Power line simulation for safety distance detection using point clouds. IEEE Access 8, 165409–165418 (2020)
13. Ma, X., Hou, F.: Research and application for transmission line sag measurement method based on aerial image sequence. DEStech Trans. Eng. Technol. Res. (2017). https://doi.org/10.12783/dtetr/iceta2016/7028
14. Jeong, Y., Kim, D., Kim, S., Ham, J.-W., et al.: Real-time environmental cognition and sag estimation of transmission lines using UAV equipped with 3-D lidar system. IEEE Trans. Power Deliv. 36(5), 2658–2667 (2021)
15. Zheng, Z., Liu, J., Zhou, B., et al.: Research on UAV sag measurement system based on 3D lidar. In: 2020 5th International Conference on Automation, Control and Robotics Engineering (CACRE), pp. 1–7. IEEE, Piscataway, NJ (2020)
16. Wang, H., Han, S., Lv, L., Jin, L.: Transmission line sag measurement based on single aerial image. In: 2017 24th International Conference on Mechatronics and Machine Vision in Practice (M2VIP), pp. 1–5. IEEE, Piscataway, NJ (2017)
17. Golinelli, E., Bartalesi, D., Ogliari, G.M., Perini, U.: A new IR laser sag meter prototype for remote on line monitoring of high voltage overhead line: A special application. In: 2019 AEIT International Annual Conference, pp. 1–6. IEEE, Piscataway, NJ (2019)
18. Golinelli, E., Perini, U., Ogliari, G.: A new IR laser scanning system for power liens sag measurements. In: 18th Italian National Conference on Photonic Technologies (Fotonica 2016), pp. 1–4. IEEE, Piscataway, NJ (2016)
19. Golinelli, E., Musazzi, S., Perini, U., Barberis, F.: Conductors sag monitoring by means of a laser based scanning measuring system: Experimental results. In: 2012 IEEE Sensors Applications Symposium Proceedings. pp. 1–4. IEEE, Piscataway, NJ (2012)
20. De Maria, L., Golinelli, E., Perini, U.: Innovative optical systems and sensors for on line monitoring of high voltage overhead lines and power components. In: 2017 AEIT International Annual Conference, pp. 1–4. IEEE, Piscataway, NJ (2017)
21. Golinelli, E., Musazzi, S., Perini, U., Pirovano, G.: Laser based scanning system for high voltage power lines conductors monitoring. In: 20th International Conference on Electricity Distribution, pp. 1–3. IEEE, Piscataway, NJ (2009)
22. Golinelli, E., Ogliari, G.M., Bartalesi, D.: New optical system for online, real time sag monitoring of high voltage overhead lines. In: 2021 AEIT International Annual Conference (AEIT), pp. 1–5. IEEE, Piscataway, NJ (2021)
23. Golinelli, E., Ogliari, G.M., Bartalesi, D.: Prototype design and preliminary tests for on line, real time sag monitoring of high voltage overhead lines. In: 2020 Italian Conference on Optics and Photonics (ICOP), pp. 1–4. IEEE, Piscataway, NJ (2020)
24. Kwinta, A., Wazydrag, y, Zygmunt, M.: Analysis of power lines span geometry based on TLS measurements. E3S Web Conf. 55, 00013 (2018)
25. Brown, F.A.: Apparatus and method of monitoring a power transmission line. US Patent, US 6,229,451 B1, 8 May 2001.
26. Moldoveanu, C., Ionita, I., Zaharescu, S., et al.: A Romanian solution for real-time monitoring of overhead transmission lines. In: 2021 9th International Conference on Modern Power Systems (MPS), pp. 1–5. IEEE, Piscataway, NJ (2021)
27. Shivani, P.G., Harshit, S., Varma, Ch.V., Mahalakshmi, R.: Detection of icing and calculation of sag of transmission line through computer vision. In: Proceedings of the Third International Conference on Smart Systems and Inventive Technology (ICSSIT 2020), pp. 689–694. IEEE, Piscataway, NJ (2020)
28. Molaei, A., Taghirad, H.D., Dargahi, J.: Extracting of sagging profile of overhead power transmission line via image processing. In: 2018 IEEE Canadian Conference on Electrical and Computer Engineering (CCECE), pp. 1–5. IEEE, Piscataway, NJ (2018)
29. Kohut, P., Holak, K., Dworakowski, Z., et al.: Vision-based measurement systems for static and dynamic characteristics of overhead lines. J. Vibroengineering 18(4), 2113–2122 (2016)
30. Abed, A., Glass, M., Trabelsi, H., Derbel, F.: Sag monitoring of overhead power lines based on image processing. In: 2021 18th International Multi-Conference on Systems, Signals & Devices (SSD'21), 142–146. IEEE, Piscataway, NJ (2021)
31. Ye, y., Tian, M., Zhang, X., et al.: The measurement of overhead conductor's sag with DLT method. In: 2nd Annual International Conference on Electronics, Electrical Engineering and Information Science (EEEIS 2016), pp. 365–371. Atlantis Press, Amsterdam, Netherlands (2016)
32. Wydra, M., Kubaczynski, P., Mazur, K., et al.: Time-aware monitoring of overhead transmission line sag and temperature with LoRa communication. Energies 12(3), 505 (2019)
33. Miralles, F., Pouliot, N., Montambault, S.: State-of-the-art review of computer vision for the management of power transmission lines. In: Proceedings of the 2014 3rd International Conference on Applied Robotics for the Power Industry, pp. 1–6. IEEE, Piscataway, NJ (2014)
34. Sermet, M.Y., Demir, I., Kucuksari, S.: Overhead power line sag monitoring through augmented reality. In: 2018 North American Power Symposium (NAPS), pp. 1–5. IEEE, Piscataway, NJ (Sept. 2018)
35. Zengin, A.T., Erdemir, G., Akinci, T.C., Seker, S.: Measurement of power line sagging using sensor data of a power line inspection robot. IEEE Access 8, 99198–99204 (2020)
36. Abraham, A.P., Ashok, S.: Gyro-accelerometric SAG analysis and online monitoring of transmission lines using line recon robot. In: 2012 Annual IEEE India Conference (INDICON), pp. 1036–1040. IEEE, Piscataway, NJ (2012)
37. Mensah-Bonsu, C., Krekeler, U.F., Heydt, G.T., et al.: Application of the global positioning system to the measurement of overhead power transmission conductor sag. IEEE Trans. Power Deliv. 17(1), 273–278 (2002)
38. Mensah-Bonsu, C.: Instrumentation and measurement of overhead conductor sag using the differential global positioning satellite system. Ph.D. Thesis, Arizona State University (2000)
39. Mensah-Bonsu, C., Heydt, G.T.: Real-time digital processing of GPS measurements for transmission engineering. IEEE Trans. Power Deliv. 18(1), 177–182 (2003)
40. Mensah-Bonsu, C., Heydt, G.T.: Overhead transmission conductor sag: a novel measurement technique and the relation of sag to real time circuit ratings. Electr. Power Compon. Syst. 31, 61–69 (2003)
41. Kamboj, S., Dahiya, R.: Application of GPS for sag measurement of overhead power transmission line. Int. J. Electr. Eng. Inform. 3(3), 268–277 (2011)
42. Kamboj, S., Dahiya, R.: Evaluation of DTLR of power distribution line from sag measured using GPS. In: 2011 International Conference on Energy, Automation and Signal, pp. 1–6. IEEE, Piscataway, NJ (2011)
43. Kamboj, S., Dahiya, R.: Case study to estimate the sag in overhead conductors using GPS to observe the effect of span length. In: 2014 IEEE PES T&D Conference and Exposition, pp. 1–4. IEEE, Piscataway, NJ (2014)

44. Mahajan, S.M., Singareddy, U.M.: A real-time conductor sag measurement system using a differential GPS. IEEE Trans. Power Deliv. 27(2), 475–480 (2012)
45. Mahajan, S.M., Singareddy, U.M.: Real time GPS data processing for sag measurement on a transmission line. In: 2008 Joint International Conference on Power System Technology and IEEE Power India Conference, pp. 1–6. IEEE, Piscataway, NJ (2008)
46. Komaragiri, S.S., Mahajan, S.M.: A sag monitoring device based on a cluster of code based GPS receivers. In: 2009 IEEE Power & Energy Society General Meeting, pp. 1–7. IEEE, Piscataway, NJ (2009)
47. Dwight, H.B.: Sag calculations for transmission lines. Trans. Am. Inst. Electr. Eng. XLV, 796–805 (1926)
48. Sakala, J.D.: Improved calculation of sag for a conductor supported at unequal heights. Int. J. Electr. Eng. Educ. 454, 327–335 (2008)
49. Ramachandran, P., Vittal, V.: On-line monitoring of sag in overhead transmission lines with levelled spans. In: 2006 38th North American Power Symposium, pp. 405–409. IEEE, Piscataway, NJ (2006)
50. Ramachandran, P., Vittal, V., Heydt, G.T.: Mechanical state estimation for overhead transmission lines with level spans. IEEE Trans. Power Syst. 23(3), 908–915 (2008)
51. He, Z., Liu, Y.: The field application analysis of dynamic line rating system based on tension monitoring. In: 2011 IEEE Power Engineering and Automation Conference, pp. 284–288. IEEE, Piscataway, NJ (2011)
52. Kumar, P., Singh, A.K.: Single measurement based mechanical state estimation for overhead transmission lines with level spans. In: ENERGYCON 2014, pp. 633–637. IEEE, Piscataway, NJ (2014)
53. Kumar, P., Singh, A.K.: Optimal mechanical sag estimator for leveled span overhead transmission line conductor. Measurement 137, 691–699 (2019)
54. McCarthy, S., Nair, N.K.C.: Final tension approximation method for determining the maximum sag of a bare overhead conductor. IET Gener. Transm. Distrib. 9(3), 249–255 (2015)
55. IEEE, IEEE Guide for Bus Design in Air Insulated Substations, IEEE Standard 605-2008 (May 2010). https://doi.org/10.1109/IEEESTD.2010.6581801
56. Abbasi, M.Z., Aman, M.A., Afridi, H.U., Khan, A.: Sag-tension analysis of AAAC overhead transmission lines for hilly areas. Int. J. Comput. Sci. Inf. Technol. Secur. 16(4), (2018)
57. Omeje, C.O., Uhunmwangho, R.: Sag and tension evaluation of a 330 kV overhead transmission line network for upland and level land topographies. Int. J. Sci. Eng. Res. 11(3), 229–234 (2020)
58. Milewski, S., Cecot, W., Orkisz, J.: On-line monitoring aided evaluation of power line cable shapes. Eng. Struct. 235, 111902 (2021)
59. Varney, T.: Aluminum Company of America, Graphic Method for Sag Tension Calculations for A1/S1A (ACSR) and Other Conductors, Pittsburg (1927)
60. Iordanescu, M., Tarnowski, J., Ratel, G., Desbiens, R.: General model for sag-tension calculation of composite conductors. In: Proceedings of the 2001 IEEE Porto Power Tech Conference. vol. 4, p. 4. IEEE, Piscataway, NJ (2001)
61. Barrett, J.S., Dutta, S., Nigol, O.: A new computer model of ACSR conductors. IEEE Trans. Power Appar. Syst. 102(3), 614–621 (1983)
62. Albizu, I., Mazon, A.J., Fernandez, E.: A method for the sag-tension calculation in electrical overhead lines. Int. Rev. Electr. Eng. 6(3, (2011)
63. Albizu, I., Mazon, A.J., Zamora, I.: Flexible strain-tension calculation method for gap-type overhead conductors. IEEE Trans. on Power Del. 24(3), 1529-1537 (2009)
64. Nash, J.F., Nash Jr, J.F.: Sag and tension calculations for cable and wire spans using catenary formulas. Electr. Eng. vol. 64(10), 685–692 (1945)
65. Winkelman, P.F.: Sag-tension computations and field measurements of Boneville Power Administration. Trans. Am. Inst. Electr. Eng. Part 3 78(4), 1532–1547 (1959)
66. Alawar, A., Bosze, E.J., Nutt, S.R.: A hybrid numerical method to calculate the sag of composite conductors. Electr. Power Syst. Res. 76, 389–394 (2006)
67. Dong, X.: Analytic method to calculate and characterize the sag and tension of overhead lines. IEEE Trans. Power Deliv. 31(5), 2064–2071 (2016)
68. CIGRE: Guide for Application of Direct Real-Time Monitoring Systems, Working Group B2.36, (2010)
69. Task Force B2.12.3, Sag-Tension Calculation Methods for Overhead Lines, CIGRE.
70. Douglass, D.A., Thrash, R.: Sag and Tension of Conductor. In: Electric Power Generation, Transmission, and Distribution: The Electric Power Engineering Handbook. pp. 15-1. CRC Press, Boca Raton, FL (2018)
71. Seppa, T.O.: Factors influencing the accuracy of high temperature sag calculations. IEEE Trans. Power Deliv. 9(2), 1079–1089 (1994)
72. Bedialauneta, M.T., Fernandez, E., Albizu, Y., et al.: Factors that affect the sag-tension model of an overhead conductor. In: 2013 IEEE Grenoble Conference, pp. 1–6. IEEE, Piscataway, NJ (June 2013)
73. Polevoy, A.: Impact of data errors on sag calculation accuracy for overhead transmission line. IEEE Trans. Power Deliv. 29(5), 2040–2045 (2014)
74. Zein, H., Utami, S., Saodah, S., Wachjoe, C.K.: Determination of overhead conductors curves with quadratic approach based. In: 2019 International Conference on Technologies and Policies in Electric Power & Energy, pp. 1–6. IEEE, Piscataway, NJ (2019)
75. Abbasi, M.Z., Noor, B., Aman, M.A., et al.: An investigation of temperature and wind impact on ACSR transmission line sag and tension. Eng. Technol. Appl. Sci. Res. 8(3), 3009–3012 (2018)
76. Alex, P., Israel, H.: Calculation of sag changes caused by conductor heating with consideration of insulator string deviation in a transmission line section. IEEE Trans. Power Deliv. 13(4), 1238–1243 (1998)
77. Gubeljak, N., Lovrencic, V., Kovac, M., et al.: Preventing transmission line damage caused by ice with smart on-line conductor monitoring. In: 2016 international conference on smart systems and technologies. pp. 155–163. IEEE, Piscataway, NJ (2016)
78. Ma, G., Li, C., Meng, C., et al.: Ice monitoring on overhead transmission lines with FBG tension sensor. In: 2010 Asia-Pacific Power and Energy Engineering Conference, pp. 1–4. IEEE, Piscataway, NJ (2010)
79. Rashmi, S., Shankaraiah, N.: An affine arithmetic approach to model and estimate the safety parameters of AC transmission lines. Int. J. Image Graph. Signal Process. 1, 11–22 (2018)
80. Abebe, Y.M., Rao, P.M.: Overhead transmission line sag, tension and length calculation using affine arithmetic. In: 2015 IEEE Power, Communication and Information Technology Conference (PCITC), pp. 211–216. IEEE, Piscataway, NJ (2015)
81. Adomah, K., Mizuno, Y., Naito, K.: Probabilistic assessment of the sag in an overhead transmission line. IEEJ Trans. Power Energy 120(10), 1298–1303 (2000)
82. Chen, S.L., Black, W.Z., Fancher, M.L.: High-temperature sag model for overhead conductors. IEEE Trans. Power Deliv. 18(1), 183–188 (2003)
83. Keshawarzian, M., Priebe, C.H.: Sag and tension calculations for overhead transmission lines at high temperatures - modified ruling span method. IEEE Trans. Power Deliv. 15(2), 777–783 (2000)
84. Kopsidas, K., Rowland, S.M., Boumecid, B.: A holistic method for conductor ampacity and sag computation on an OHL structure. IEEE Trans. Power Deliv. 27(3), 1047–1054 (2012)
85. de Nazare, F.V.B., Werneck, M.M.: Development of a monitoring system to improve ampacity in 138kV transmission lines using photonic technology. In: IEEE PES T&D 2010, pp. 1–6. IEEE, Piscataway, NJ (2010)
86. de Nazare, F.V.B., Werneck, M.M.: Hybrid optoelectronic sensor for current and temperature monitoring in overhead transmission lines. IEEE Sens. J. 12(5), 1193–1194 (2012)
87. Hatibovic, A.: Derivation and analysis of the relation between conductor sags in inclined and levelled spans based on known data of the latter. B2-202, CIGRE (2014)
88. Liu, Y., Zhang, L., Wang, J.: Computation of standard sag of overhead lines for power grid based on mathematical model of iterative technique. In: 2010 2nd International Conference on Computer Engineering and Technology, pp. V1-445–V1-448. IEEE, Piscataway, NJ (2010)
89. Xiao, X., Xu, Y., Zhang, J., Xu, K.: Research on sag online monitoring system for power transmission wire based on tilt measurement. Int. J. Smart Grid Clean Energy 2(1), 6–11 (2013)

90. D. Sacedotianu, Nicola, M., et al.: Research on the continuous monitoring of the sag of overhead electricity transmission cables based on the measurement of their slope. In: 2018 International Conference on Applied and Theoretical Electricity (ICATE), pp. 1–5. IEEE, Piscataway, NJ (2018)
91. Hayes, R.M., Nourai, A.: Power line sag monitor, US Patent 6,205,867 B1, 27 March 2001
92. Malhara, S., Vittal, V.: Mechanical state estimation of overhead transmission lines using tilt sensors. IEEE Trans. Power Syst. 25(3), 1282–1290 (2010)
93. Gong, X., Wang, Z., Xu, W., et al.: Research on online sag monitoring of transmission lines based on barometric pressure. IOP Conf. Ser.: Earth Environ. Sci. 791, 012094 (2021)
94. Mamishev, A.V., Nevels, R.D., Russel, B.D.: Effects of conductor sag on spatial distribution of power line magnetic field. IEEE Trans. Power Deliv. 11(3), 1571–1576 (1996)
95. Halverson, P.G., Syracuse, S.J., Clark, R., Tesche, F.M.: Non-contact sensor system for real-time high-accuracy monitoring of overhead transmission lines. Proc. Epri Conf. Overhead Trans. Lines 1-13 (2008)
96. Promethean Devices LLC, Sensor, Method and System of Monitoring Transmission Lines, US Patent, 8,280,652 B2, 10 Feb 2012
97. Sun, X., Lui, K.S., Wong, K.K.Y., et al.: Novel application of magnetoresistive sensors for high-voltage transmission-line monitoring. IEEE Trans. Magn. 47(10), 2608–2611 (2011)
98. Sun, X., Huang, Q., Hou, Y., Jiang, L., Pong, P.W.T.: Noncontact operation-state monitoring technology based on magnetic-field sensing for overhead high-voltage transmission lines. IEEE Trans. Power Deliv. 28(4), 2145–2153 (2013)
99. Khawaja, A.H., Huang, Q.: Characteristic estimation of high voltage transmission line conductors with simultaneous magnetic field and current measurements. In: 2016 IEEE International Instrumentation and Measurement Technology Conference Proceedings, pp. 1–6. IEEE, Piscataway, NJ (2016)
100. Khawaja, A.H., Huang, Q.: Estimating sag and wind-induced motion of overhead power lines with current and magnetic-flux density measurements. IEEE Trans. Instrum. Meas. 66(5), 897–909 (2017)
101. Khawaja, A.H., Huang, Q., Li, J., Zhang, Z.: Estimation of current and sag in overhead power transmission lines with optimized magnetic field sensor array placement. IEEE Trans. Magn. 53(5), 1–10 (2017)
102. Xu, Q., Liu, X., Zhu, K., Pong, P.W.T., Liu, C.: Magnetic-field-sensing-based approach for current reconstruction, sag detection, and inclination detection for overhead transmission system. IEEE Trans. Magn. 55(7), (2019)
103. Fan, H., Huang, Q., Zhang, Z., et al.: A novel non-contact measurement method for current positioning based on magnetic sensors. In: 2021 IEEE/IAS Industrial and Commercial Power System Asia, pp. 1518–1524. IEEE, Piscataway, NJ (2021)
104. Kitic, N., Matic, P.: Approximate magnetic flux density model of overhead power lines for conductor sag estimation. Int. J. Electr. Comput. Eng. 5(2), 69–76 (2021)
105. Kiti, N., Mati, P., Leki, D., et al.: Real-time sag estimation of overhead power lines based on approximate magnetic field model. In: 2022 21st International Symposium INFOTEH-JAHORINA (INFOTEH), pp. 1-6. IEEE, Piscataway, NJ (2022)
106. Mahin, A.U., Hossain, M.F.: Millimeter wave based sag measurement technique for overhead transmission lines in smart-grid. International Conference on Energy and Power Engineering, pp. 1–5. IEEE, Piscataway, NJ (2019)
107. Mahin, A.U., Islam, S.N., Hossain, M.F.: Millimeter wave based sag measurement using parabolic approximation for smart grid overhead transmission line monitoring. In: 2019 IEEE International Conference on Communications, Control, and Computing Technologies for Smart Grids (SmartGridComm), pp. 1–5. IEEE, Piscataway, NJ (2019)
108. Mahin, A.U., Hossain, M.F., Islam, S.N., et al.: Millimeter wave based real-time sag measurement and monitoring system of overhead transmission lines in a smart grid. IEEE Access 8, 100754–100767 (2020)
109. Mahin, A.U.: Design of millimeter wave based sag measurement and monitoring system for overhead transmission lines in a smart grid. M.Sc. Thesis, Bangladesh University of Engineering and Technology (2019).
110. Hlalele, T.S., Du, S.: Radio technology frequency identification applied in high-voltage power transmission-line for sag measurement. Int. J. Electr. Comput. Eng. Syst. 7(7), 928–932 (2013)
111. Hlalele, T.S.: Radio frequency identification for the measurement of overhead power transmission line conductor sag. Master Thesis, University of South Africa (2015)
112. Jiang, J.J., Chiu, H.-C., Yang, Y.-C., et al.: On real-time detection of line sags in overhead power grids using an IoT-based monitoring system: theoretical basis, system implementation, and long-term field verification. IEEE Internet Things J. 9(15), 13096–13112 (2022)
113. Hsu, T.S., Chiu, H.C., Yang, Y.C., et al.: An IoT-based sag monitoring system for overhead transmission lines. In: 2019 IEEE PES GTD Grand International Conference and Exposition Asia (GTD Asia), pp. 515–519. IEEE, Piscataway, NJ (2019)
114. Saradhi, M.V.V., Nagaraju, S.: Development of a low-cost ZIGBEE and GSM SMS-based conductor temperature and sag monitoring system. Int. J. Eng. Res. Technol. 2(4), 372–381 (2010)
115. Yaroslavsky, D., Nguyen, V.V., Sadykov, M., et al.: Determination the conductor sag according to the period of own harmonic oscillations. E3S Web of Conferences 220, 01036 (2020)
116. Yaroslavsky, D. A., Nguyen, V.V., et al.: Studying the model of free harmonic oscillations of overhead power lines. Int. J. Emerging Trends Eng. Dev. 8(6), 2663–2667 (2020)
117. Mendrok, K., Dworakowski, Z., Holak, K., Kohut, P.: Application of vision measurements for modal analysis of wires for the purpose of overhead transmission lines monitoring. J. Phys.: Conf. Ser. 842, 012011 (2017)
118. Cloet, E., Lilien, J.-L., Ferrieres, R.: Experiences of the Belgian and French TSOs using the Ampacimon real-time dynamic rating system, C2_106_2010. pp. 1–8. Conseil International des Grands Reseaux Electriques, Paris (2010)
119. Cloet, E., Lilien, J.-L.: Uprating transmission lines through the use of an innovative real-time monitoring system. In: 2011 IEEE PES 12th International Conference on Transmission and Distribution Construction, Operation and Live-Line Maintenance (ESMO), pp. 1–6. IEEE, Piscataway, NJ (2011)
120. Mukherjee, M., Olsen, R.G., Li, Z.: Non-contact monitoring of overhead transmission lines using space potential phasor measurements. IEEE Trans. Instrum. Meas. 69(10), 7494–7504 (2020)
121. Ji, Y., Yuan, J.: Overhead transmission lines sag and voltage monitoring method based on electrostatic inverse calculation. IEEE Trans. Instrum. Meas. 71, 9002312 (2022)
122. El Dein, A.Z., Wahab, M.A.A., Hamada, J.J., Emmary, T.H.: The effects of the span configurations and conductor sag on the electric-field distribution under overhead transmission lines. IEEE Trans. Power Deliv. 25(4), 2891–2902 (2010)
123. Saied, M.M.: On the sag monitoring for the dynamic rating of overhead power lines. Paper presented at proceedings international conference on condition monitoring and diagnosis, Changwon, South Korea, 2–5 April 2006.
124. Olsen, R.G., Edwards, K.S.: A new method for real-time monitoring of high-voltage transmission-line conductor sag. IEEE Trans. Power Deliv. 17(4), 1142–1152 (2002)
125. Oleinikova, I., Mutule, A., Putnins, M.: PMU measurements application for transmission line temperature and sag estimation algorithm development. In: 2014 55th International Scientific Conference on Power and Electrical Engineering of Riga Technical University (RTUCON), pp. 181–185. IEEE, Piscataway, NJ (2014)
126. Du, Y., Liao, Y.: On-line estimation of transmission line parameters, temperature and sag using PMU measurements. Electr. Power Syst. Res. 93, 39–45 (2002)
127. Du, Y., Liao, Y.: Online estimation transmission parameters temperature sag. In: 2011 North American Power Symposium, pp. 1–6. IEEE, Piscataway, NJ (2011)

128. de Villiers, W., Cloete, J.H., Wedepohl, L.M., Burger, A.: Real-time sag monitoring system for high-voltage overhead transmission liens based on power-line carrier signal behavior. IEEE Trans. Power Deliv. 23(1), 389–395 (2008)
129. de Villiers, W.: Real-time HV OHTL Sag Monitoring System Based on Power Line Carrier Signal Behaviour. Ph.D. Thesis, University of Stellenbosch (2005)
130. Wydra, M., Kisala, P., Harasim, D., Kacejko, P.: Overhead transmission line sag estimation using a simple optomechanical system with chirped fiber Bragg gratings part 1: Preliminary measurements. Sensors 18(1), 309 (2018)
131. Skorupski, K., Harasim, D., Panas, P., et al.: Overhead transmission line sag estimation using the simple opto-mechanical system with fiber Bragg gratings Part 2: Interrogation system. Sensors 20(9), 2652 (2020)
132. Gangopadhyay, T.K., Paul, M.C., Bjerkan, L.: Fiber-optic sensor for real-time monitoring of temperature on high voltage (400 KV) power transmission lines. Proc. SPIE 7503, 75034M (2009)
133. Ding, Z.-W., Zhang, X.-P., Zou, N.-M., et al.: Phi-OTDR based on-line monitoring of overhead power transmission line. J. Light. Technol. 39(15), 5163–5169 (2021)
134. Huang, J., Bo, R.: Real-time Overhead Power Line Sag Monitoring, International Patent, WO 2019/126020 A1, (2019)
135. Bush, R.A., Black, W.Z., Champion III, T.C., Byrd, W.R.: Experimental verification of a real-time program for the determination of temperature and sag of overhead lines. IEEE Trans. Power Appar. Syst. PAS-102(7), 2284–2288 (1983)
136. Ren, L., Li, H., Liu, Y.: On-line monitoring and prediction for transmission line sag. In: 2012 IEEE International Conference on Condition Monitoring and Diagnosis, pp. 813–817. IEEE, Piscataway, NJ (2012)
137. Balango, D., Nemeth, B.: Predicting conductor sag of power lines in a new model of dynamic line rating. In: 2015 Electrical Insulation Conference (EIC), pp. 41–44. IEEE, Piscataway, NJ (2015)
138. Liao, R., Liao, J., Zhang, Y., et al.: Sag prediction of high-voltage transmission lines based on PSO-SVM. In: 2020 35th Youth Academic Annual Conference of Chinese Association of Automation (YAC), pp. 772–777. IEEE, Piscataway, NJ (2020)
139. Mahin, A.U., Islam, S.N., Ahmed, F., Hossain, M.F.: Measurement and monitoring of overhead transmission line sag in smart grid: A review. IET Gener. Transm. Distrib. 16(1), 1–18 (2021)
140. Khawaja, A.H., Huang, Q., Khan, Z.H.: Monitoring of overhead transmission lines - a review from perspective of contactless technologies. Sens. Imaging 18, 24 (2017)
141. Zaihuddin, N., Rahman, M.S.A., Kadir, M.Z.A.Ab., et al.: Review of thermal stress and condition monitoring technologies for overhead transmission lines: Issues and challenges. IEEE Access 8, 120053–120081 (2020)
142. Hlalele, T.S., Du, S.: Real time monitoring of high voltage transmission line conductor sag: the state-of-the-art. Int. J. Eng. Adv. Technol. 3(1), 297–303 (2013)
143. EPRI: Video sagometer application guide. Technical report 1001921, 129 (2001)
144. USi-Power Inc.: Donut® Line Monitor. http://www.usi-power.com/power-donut-line-monitor/. Accessed 31 Oct 2022
145. USI-Power Inc.: Power Donut2 System for Overhead Transmission Line Monitoring. Product overview. http://www.usi-power.com/power-donut-line-monitor/ (2006)
146. USI-Power Inc.: Power Donut2 System for Overhead Transmission Line Monitoring. Communications brochure. http://www.usipower.com/Product%20&%20Services/Donut/PowerDonut2%20Cell.pdf. Accessed 31 Oct 2022
147. Power Line Systems Inc., Apparatus and method of monitoring a power transmission line. US Patent 6,229,451, 20 Feb 1997
148. The Valley Group Inc.: CAT - 1 Transmission Line Monitoring System, Brochure. http://www.cat-1.com/files/brochures/CAT-1.pdf. Accessed 31 Oct 2022
149. EDM International, Inc.: Sagometer. Product Overview. http://edmlink.com/EMD_Sagometer.pdf. Accessed 31 Oct 2022
150. IEEE Power and Energy Society Transmission and Distribution Committee: IEEE guide for the installation of overhead transmission line conductors. In: IEEE Standard 524 -2016, pp. 1–162. IEEE, Piscataway, NJ (2016)

How to cite this article: Chen, Y., Ding, X.: A survey of sag monitoring methods for power grid transmission lines. IET Gener. Transm. Distrib. 17, 1419–1441 (2023). https://doi.org/10.1049/gtd2.12778